**THE EUROPEAN
PHYSICAL JOURNAL C**

Dark energy and accelerating cosmological evolution from osculating Barthel–Kropina geometry

Rattanasak Hama[1,a], **Tiberiu Harko**[2,3,4,b], **Sorin V. Sabau**[5,6,c]

[1] Faculty of Science and Industrial Technology, Prince of Songkla University, Surat Thani Campus, Surat Thani 84000, Thailand
[2] Department of Theoretical Physics, National Institute of Physics and Nuclear Engineering (IFIN-HH), 077125 Bucharest, Romania
[3] Department of Physics, Babes-Bolyai University, Kogalniceanu Street, 400084 Cluj-Napoca, Romania
[4] Astronomical Observatory, 19 Ciresilor Street, 400487 Cluj-Napoca, Romania
[5] Department of Biology, School of Biological Sciences, Tokai University, Sapporo 005-8600, Japan
[6] Graduate School of Science and Technology, Physical and Mathematical Sciences, Tokai University, Sapporo 005-8600, Japan

Abstract Finsler geometry is an important extension of Riemann geometry, in which each point of the spacetime manifold is associated with an arbitrary internal variable. Two interesting Finsler geometries with many physical applications are the Randers and Kropina type geometries. A subclass of Finsler geometries is represented by the osculating Finsler spaces, in which the internal variable is a function of the base manifold coordinates only. In an osculating Finsler geometry, we introduce the Barthel connection, with the remarkable property that it is the Levi–Civita connection of a Riemannian metric. In the present work we consider the gravitational and cosmological implications of a Barthel–Kropina type geometry. We assume that in this geometry the Ricci type curvatures are related to the matter energy–momentum tensor by the standard Einstein equations. The generalized Friedmann equations in the Barthel–Kropina geometry are obtained by considering that the background Riemannian metric is of Friedmann–Lemaitre–Robertson–Walker type. The matter energy balance equation is also derived. The cosmological properties of the model are investigated in detail, and it is shown that the model admits a de Sitter type solution and that an effective dark energy component can also be generated. Several cosmological solutions are also obtained by numerically integrating the generalized Friedmann equations. A comparison of two specific classes of models with the observational data and with the standard ΛCDM model is also performed, and it is found that the Barthel–Kropina type models give a satisfactory description of the observations.

[a] e-mail: rattanasak.h@psu.ac.th
[b] e-mail: tiberiu.harko@aira.astro.ro (corresponding author)
[c] e-mail: sorin@tokai.ac.jp

Contents

Springer

1 Introduction

Finsler geometry [1–6] is a well-studied generalization of the Riemann geometry which is constructed from the general line element $ds = F\left(x^1, x^2, \ldots, x^n; dx^1, dx^2, \ldots, dx^n\right) = F(x, y)$, where $F(x, y) > 0$, $\forall y \neq 0$, is a function on the tangent bundle $T(M)$, and homogeneous of degree 1 in y. In fact, however, Finsler geometry is not just an extension of Riemannian geometry, but it is Riemannian geometry without the quadratic line element restriction [7]. If in Riemannian geometry $F^2 = g_{IJ}(x)dx^I dx^J$ [8], in a Finsler geometry the differential line element ds at x in general is a function of both x and y, and it is defined according to $\sqrt{d\mathbf{x} \cdot d\mathbf{x}} = \left[g_{AB}(x, y)dx^A dx^B\right]^{1/2}$, respectively. In the present paper, capital Latin indices take values in the range $(0, 1, 2, 3)$, while small Latin letters take values in the range $(1, 2, 3)$. Finsler spaces have a much richer mathematical structure than their Riemannian counterparts. In a Finsler space, one can define three kinds of curvature tensors $\left(R^\kappa_{\nu\lambda\mu}, S^\kappa_{\nu\lambda\mu}, P^\kappa_{\nu\lambda\mu}\right)$, and five torsion tensors [5], which shows that Finsler geometry indeed has a higher degree of complexity than Riemann geometry.

Finsler spaces have a large number of physical applications. Randers [9] unified theory of gravity and electromagnetism, initially constructed in the framework of five-dimensional general relativity, proved to be an example of a Finsler geometry, with $ds = (\alpha + \beta)du$, where $\alpha = \left[g_{IK}(x)y^I y^K\right]^{1/2}$, and $\beta = b_I(x)y^I$, where $y^I = dx^I/du$. Quantum mechanics in its hydrodynamical formulation can also be interpreted in terms of Finslerian geometry [10–13].

The Einstein gravitational field equations, $G_{\mu\nu} = R_{\mu\nu} - (1/2)Rg_{\mu\nu} = \kappa^2 T_{\mu\nu}$, where $R_{\mu\nu}$ is the contraction of the Riemann curvature tensor, $R_{\mu\nu} = R^\kappa_{\mu\kappa\nu}$, R is the Ricci scalar $R = R^\mu_\mu$, $T_{\mu\nu}$ is the matter energy–momentum tensor, and $\kappa^2 = 8\pi G/c^4$ is the gravitational coupling constant, are the mathematical representation of one of the most beautiful and successful physical theories ever proposed: general relativity. However, general relativity has recently begun to face a number of strong theoretical challenges. The data obtained from the observations of the type Ia supernovae in [14–20] suggest that the universe is at present in an accelerated, de Sitter type expansionary phase. These observations have led to many observational and theoretical works trying to understand the present-day cosmological dynamics (for a review of the cosmic acceleration problem see [21]). The Planck satellite studies of the cosmic microwave background [22], together with the investigations of baryon acoustic oscillations [23–25], also confirmed the accelerating expansion of the universe. But to explain these remarkable discoveries, we need a fundamental change in our present understanding of the gravitational interaction. The simplest explanation for the accelerated expansion is obtained by reintroducing in the gravitational field equations the cosmological constant Λ proposed by Einstein in 1917 [26] to obtain a static model of the cosmos. The Einstein field equations together with the cosmological constant provide very good fits to all the observational data, but with the very high price of introducing a parameter whose physical (or geometric) nature is not (yet) known (for detailed discussions on the cosmological constant problem see [27–29]. Hence, in order to solve some of the theoretical problems of cosmology without resorting to the cosmological constant, the existence of a new essential component of the universe, called dark energy, was postulated. Many dark energy models have been proposed (for extensive reviews see [30–35]). Perhaps the simplest dark energy model can be constructed by using a single scalar field, ϕ, in the presence of a self-interaction potential $V(\phi)$, with the gravitational action given by

$$S = \int \left[\frac{M_p^2}{2}R - (\partial\phi)^2 - V(\phi)\right]\sqrt{-g}\,d^4x, \qquad (1)$$

where R is the Ricci scalar, and M_p denotes the Planck mass. The dark energy models obtained in this way are called quintessence models [36–40].

The dark matter problem represents another fundamental problem in present-day astrophysics and cosmology (see [41–43] for detailed reviews of the recent results on the search for dark matter, and for its properties). The presence of dark matter at galactic and extragalactic scales is required to obtain an explanation of two basic astrophysical/astronomical observations, the behavior of the galactic rotation curves and the virial mass problem in clusters of galaxies, respectively. The observations of the galactic rotation curves [44–47] convincingly show that neither Newtonian gravity nor Einstein's general relativity can describe galactic dynamics. To explain the properties of the galactic rotation curves and to solve the missing mass problem in clusters of galaxies, it is necessary to postulate the existence of a dark (invisible) component of the universe that interacts only gravitationally with baryonic matter, and which resides in a spherically symmetric halo around the galaxies. Usually, dark matter is described as a cold, pressureless cosmic fluid. Many candidates have been proposed for the dark matter particle, including weakly interacting massive particles (WIMPs), axions, neutrinos, gravitinos, and neutralinos (for

extensive reviews of the dark matter particle candidates see [48–51]). Dark matter particles interact with normal baryonic matter very weakly; however, their interaction cross sections are expected to be nonzero. Thus, their direct experimental detection in laboratory experiments may be possible.

Therefore, in the present-day view of the cosmological evolution, the local dynamics and the global expansion of the universe are dominated by two major components, dark energy and cold dark matter, respectively, with baryonic matter playing an insignificant role in late-time cosmological evolution. The simplest theoretical model which can fully explain the late-time accelerating de Sitter expansion is obtained by reintroducing in the Einstein gravitational field equations the cosmological constant Λ. The Λ extension of the Einstein gravitational field equations represents the theoretical foundation of the currently dominant standard cosmological paradigm, the Λ cold dark matter (ΛCDM) model, with cold dark matter also playing a fundamental role. Despite its theoretical simplicity, the ΛCDM model fits the cosmological observations very well [52–55].

However, apart from its theoretical and fundamental aspects, the ΛCDM model is also confronted with some interesting (and as yet unsolved) observational problems. The most important of these problems is the "Hubble tension," which originated from the important differences obtained between the numerical values of the Hubble constant, H_0, as determined by the Planck satellite from the measurements of the cosmic microwave background (CMB) [55], and the values measured directly by using cosmological and astrophysical observations in the local universe [56–58]. To illustrate the differences, the SH0ES determinations of H_0 give the value $H_0 = 74.03 \pm 1.42$ km/s/Mpc [56], while the analysis of the CMB, originating in the early universe, gives, via the Planck satellite data, $H_0 = 67.4 \pm 0.5$ km/s/Mpc [54], a value differing from the SH0ES result by $\sim 5\sigma$.

Hence, the search for alternative explanations for the cosmological dynamics and the nature of the two mysterious major components of the universe is a critical task for present-day theoretical physics. One of the attractive possibilities for solving the gravitational puzzles is to go beyond the framework of the Riemannian geometry on which general relativity is constructed, and look for more general geometries that could describe the intricate nature of the gravitational phenomena. In this direction, one very promising candidate is Finsler geometry.

Horváth [59] and Horváth and Moór [60] were the first to attempt to formulate a relativistic theory of gravitation by using Finsler geometry, with their work later extended in [61] and [62], respectively. The physical and cosmological implications of the Finsler geometry have been investigated from different points of view in [63–100]. In particular, in [100], the cosmological evolution in an osculating point Barthel–Randers type geometry was considered. In this type of geometry, each point of the spacetime manifold is associated with an arbitrary point vector field. For the Barthel–Randers geometry, the connection is given by the Levi–Civita connection of the associated osculating Riemann metric. This Finsler type geometry is assumed to describe the physical properties of the gravitational field via the standard Einstein equations, as well as the cosmological dynamics. The generalized Friedmann equations in the Barthel–Randers geometry were obtained by considering that the background Riemannian metric in the Randers line element is of Friedmann–Lemaître–Robertson–Walker type. The matter energy balance equation was obtained, and it was investigated from the perspective of the thermodynamics of irreversible processes in the presence of particle creation. The cosmological properties of the Barthel–Randers model were investigated in detail, and it was shown that the model permits a de Sitter type solution, and that an effective cosmological constant can also be generated. Several exact cosmological solutions were also obtained, and a comparison of three specific models with the observational data and with the standard ΛCDM model was performed by fitting the observed values of the Hubble parameter. It turns out that the Barthel–Randers models give a satisfactory description of the observations.

Alternative mathematical formulations within a Finsler geometric framework are also possible. For example, in [91] the cosmological implications of scalar–tensor theories that are effectively obtained from the Lorentz fiber bundle of a Finsler-like geometry were investigated. In this approach, it is assumed that in the Finsler space one can define a nonlinear connection with local components $N_\mu^{(\alpha)}\left(x^\nu, \phi^{(\beta)}\right)$, where $\left(x^\nu, \phi^{(\beta)}\right)$ are the local coordinates, with x^ν, $\nu = 0, \ldots 3$, the coordinates on the local manifold, and $\phi^{(\beta)}$, $\beta = 1, 2$ the coordinates on the fiber. The nonlinear connection uniquely splits the total space TE into a horizontal distribution HE and a vertical distribution VE, so that $TE = HE \oplus \oplus VE$. The metric tensor can then be constructed as

$$G = g_{\mu\nu}(x)\mathrm{d}x^\mu \otimes \mathrm{d}x^\nu + v_{(\alpha)(\beta)}(x)\delta\phi^{(\alpha)} \otimes \delta\phi^{(\beta)}, \qquad (2)$$

where for $g_{\mu\nu}$ a Lorentzian signature $(-, +, +, +)$ was adopted, with the fiber variables $\phi^{(\alpha)}$ playing the role of internal variables. The gravitational field equations are obtained from a variational principle, with the action constructed as $S = (1/16\pi G) \int \sqrt{|G|}L_G \mathrm{d}x^{(N)}$, where $\mathrm{d}x^{(N)} = \mathrm{d}^4x \wedge \mathrm{d}\phi^{(1)} \wedge \mathrm{d}\phi^{(2)}$. For the Lagrangian density, two forms were considered, the first being $L_G = \tilde{R} - V(\phi)/\phi$, where $\tilde{R} = R - 2\Box\phi/\phi + \partial_\mu\phi\partial^\mu\phi/2\phi^2$ is the curvature for the case of a holonomic basis, and $V(\phi)$ is the scalar field potential. A second possible choice considered in [91] is $L_G = \bar{R}$, where $\bar{R}$ is the curvature of a non-holonomic basis. Matter can also be added to the gravitational action, and thus the total action becomes

$$S = \frac{1}{16\pi G} \int \sqrt{|\det g|}\phi L_G dx^{(N)} + \int \sqrt{|\det g|}\phi L_M dx^{(N)},$$

$$(3)$$

where L_M is the matter Lagrangian. By using both choices of action, the cosmological implications of the model were investigated, and it was shown that an effective dark energy sector does appear from the geometric structure of the Finsler model. Moreover, an explicit interaction between the matter and dark energy sectors is generated. As applied to the cosmological evolution of the universe, it was shown that one can obtain a sequence of successive matter- and dark energy-dominated epochs, with the parameter of the equation of state of the dark energy being quintessence-like, phantom-like, or experiencing the phantom-divide crossing. An exponential de Sitter solution can also be obtained.

A generalized scalar–tensor theory obtained from vector bundle constructions was considered in [98], where its kinematic, dynamical, and cosmological consequences were studied. The theory is characterized by a mathematical structure constructed over a pseudo-Riemannian spacetime base manifold, together with a fiber structure with two scalar fields. Hence, one obtains a six-dimensional vector bundle endowed with a nonlinear connection as the geometric arena for the description of the gravitational interaction. The geodesics and the Raychaudhuri and field equations are obtained using both the Palatini and the metric approach. For the cosmological metric, we adopt the expression [98]

$$G = -dt \otimes dt + a^2(t)\left(dx \otimes dx + dy \otimes dy + dz \otimes dz\right)$$
$$+ \phi(t)\left(\delta\phi^{(1)} \otimes \delta\phi^{(1)} + \delta\phi^{(2)} \otimes \delta\phi^{(2)}\right),$$

$$(4)$$

and the corresponding Friedmann equations become [98]

$$3H^2 = 8\pi G \left(\rho_m + \rho_{eff}\right),$$

$$(5)$$

$$2\dot{H} = -8\pi G \left(\rho_m + \rho_{eff} + p_m + p_{eff}\right),$$

$$(6)$$

where

$$\rho_{eff} = \frac{1}{8\pi G}\left[\frac{\dot{\phi}}{\phi}W_+ - \frac{\dot{\phi}^2}{4\phi^2} - 3H\left(\frac{\dot{\phi}}{\phi} - W_+\right)\right],$$

$$(7)$$

and

$$p_{eff} = \frac{1}{8\pi G}\left[(W_+)^2 - \dot{W}_+ - 2HW_+ - \frac{\dot{\phi}^2}{4\phi^2}\right.$$
$$\left. + \frac{1}{2\phi}\left(4H\dot{\phi} - 3W_+\dot{\phi} + \ddot{\phi}\right)\right],$$

$$(8)$$

respectively, where W_+ is the contribution coming from the non-diagonal components of the field equations. Hence, the Finsler geometric structure generates extra terms in the modified Friedmann equations corresponding to an effective dark energy sector, also leading to an interaction of the dark matter sector with the metric. The parameter of the dark energy equation of state can take values in either the quintessence or the phantom regime, or that indicate the phantom-divide crossing.

It is the goal of the present paper to extend the investigations of the cosmological properties of the Finsler spaces, as initiated in [100], by considering a systematic investigation of another Finsler type geometry which is based on the Kropina metric [101,102], a particular class of the general (α, β) metrics with $F = \alpha^2/\beta$. The Randers metric also belongs to the class of (α, β) metrics. We assume that the true description of the gravitational interaction can be accomplished by using the mathematical properties of the Kropina spaces in a mathematical framework introduced by Barthel [103,104], in which one can consider a Finsler space as an n-dimensional point space which is locally Minkowskian (a space that is flat, homogeneous, and anisotropic) but, in general, is not locally Euclidean. Note that a general Finsler space is both inhomogeneous and anisotropic.

The starting point of the theory of the gravitational interaction based on the point Finsler spaces is the assumption that the gravitational field can be represented by a Riemannian metric $g(x)$, satisfying the Einstein gravitational field equations. The next step in the construction of a Finsler type gravitational theory is the non-localization (anisotropization) of the background geometry, by attaching to each point $x = (x^I)$, $I = 0, 1, 2, 3$, an internal variable $y = (y^J)$, $J = 0, 1, 2, 3$. Under the assumption that y is a vector, the nonlocal gravitational field can be described by using a Finsler type geometry F^4 or, alternatively, by the geometry of a general vector bundle. *In nonlocal Finslerian geometry, the metric tensor depends on both the local coordinates x and the vector y, so that $\hat{g} = \hat{g}(x, y)$.*

However, for many realistic physical processes, one can assume that the variable y is a function of the position $y = Y(x)$. Thus, the Finslerian metric becomes $\hat{g} = \hat{g}(x, Y(x))$. Hence, in this particular type of physical model, the Finslerian metric tensor $\hat{g}$b is a function only of x. In this way, we define a manifold called the osculating Finsler manifold. The geometric properties of the osculating Finsler space are described by using the Barthel connection [103,104]. In the case of the Kropina geometry (as well as in all (α, β) geometries) we have the remarkable result that the Barthel connection is the Levi–Civita connection of the Riemannian metric $\hat{g}(x, y(x))$. In the present work we systematically and rigorously investigate the cosmological implications of the Barthel–Kropina geometry by adopting for the background Riemann metric the Friedmann–Lemaître–Robertson–Walker (FLRW) form. In the Barthel–Kropina-FLRW geometry we obtain the generalized Friedmann equations of the model. The properties of the cosmological equations are investigated in detail, and several evolutionary scenarios are constructed, describing different

types of dynamics. The model admits a de Sitter type solution, describing an accelerating universe but in the presence of nonzero matter density. Different cosmological solutions corresponding to particular choices of the coefficients of the one-form β are also considered, and their behavior is compared with the observational data as well as with the predictions of the standard ΛCDM model. An effective dark energy model can also be generated from the generalized Friedmann equations, and its properties are analyzed in detail. Decelerating solutions can also be obtained, and they may provide, for example, alternative descriptions to the radiation-dominated phase of standard cosmology. The overall comparison of the considered models with the observational data indicates that they provide a satisfactory description of the cosmological dynamics, at least on a qualitative level.

The present paper is organized as follows. In Sect. 2, we review the necessary elements and definitions of the Finsler geometry and point and osculating Finsler spaces. The Barthel connection is also introduced in an intuitive way. General definitions of the curvature tensors are also presented, and the specific form of the Einstein gravitational field equations is postulated. The cosmological framework involving the definitions of the Riemann metric, the one-form β, and the thermodynamic parameters is constructed in Sect. 3. The Finslerian metric tensor coefficients, the Christoffel symbols, and the curvature tensors are obtained for the considered geometry. Based on this, geometric results are derived for the generalized Friedmann equations describing the cosmological evolution in the Barthel–Kropina-FLRW geometry. Particular cosmological models are considered in Sect. 4. It is shown that the model admits a de Sitter type solution, in the presence of a nonzero matter density. Cosmological models corresponding to two specific choices of the function η, giving the only nonzero coefficient of the one-form β, are considered in detail. The predictions of the model with a specific dependence on the Hubble function of β are compared with observational data and the standard ΛCDM model. The possibility of obtaining an effective dark energy model equivalent to a time-varying cosmological constant is analyzed in Sect. 5. We discuss our results and presents conclusions in Sect. 6. The calculations of all the geometric quantities are presented in five appendices. In Appendix A, the details of the computation of the Finsler metric tensor are explicitly shown. The expressions of the Christoffel symbols in the Barthel–Kropina-FLRW geometry are derived in Appendix B. The components of the Ricci tensors are obtained in Appendix C. The Ricci scalar is computed in Appendix D. Finally, the explicit computations leading to the Einstein gravitational field equations and to the generalized Friedmann equations are presented in Appendix E.

2 A brief review of the Finsler, (α, β), and Barthel–Kropina geometries

In the present section we will briefly introduce the basics of the Finsler geometry, the (α, β)-metrics, the Barthel connection, and the Barthel–Kropina geometry.

It is important to emphasize that Finsler geometry already appears in classical Newtonian mechanics when dissipative effects are present. If the equations of motion of a dynamical system, defined on an n-dimensional differentiable manifold M, can be obtained from a regular Lagrangian L via the Euler–Lagrange equations, given by

$$\frac{d}{dt}\frac{\partial L}{\partial y^i} - \frac{\partial L}{\partial x^i} = F_i, \, i \in \{1, 2, \ldots, n\}, \tag{9}$$

where F_i are the external forces, the above Euler–Lagrange equations are equivalent to a system of second-order differential equations of the form

$$\frac{d^2 x^i}{dt^2} + 2G^i\left(x^j, y^j, t\right) = 0, \, i \in \{1, 2, \ldots, n\}, \tag{10}$$

where each function $G^i\left(x^j, y^j, t\right)$ is C^∞ in Ω in the neighborhood of some initial conditions $\left((x)_0, (y)_0, t_0\right)$. Equation (10) can naturally be interpreted as describing geodesic motion in a Finsler space.

2.1 Finsler geometry and particular Finsler spaces

A basic assumption of the present-day theoretical physics is that space and time are unified in a single structure (the spacetime) that can be described mathematically as a four-dimensional differentiable manifold M, endowed with a pseudo-Riemannian metric tensor g_{IJ}, where $I, J, K \ldots = 0, 1, 2, 3$. On the world line of a standard clock, the spacetime interval between two events x^I and $x^I + dx^I$ is given, according to the chronological hypothesis, by $ds = \left(g_{IJ}dx^I dx^J\right)^{1/2}$ [105,106]. But from a mathematical point of view, one can go beyond the Riemannian mathematical structures of the spacetime manifold. One of the most important metric extensions of the Riemann geometry is the geometry introduced by Finsler [1–6].

From a general mathematical point of view, Finsler spaces are metric spaces in which the interval ds between two nearby points $x = (x^I)$ and $x + dx = (x^I + dx^I)$ is given by

$$d\hat{s} = F(x, dx), \tag{11}$$

where F, the Finsler metric function, is positively homogeneous of degree 1 in dx, and thus has the property

$$F(x, \lambda dx) = \lambda F(x, dx). \tag{12}$$

To permit the use of local coordinates in mathematical computations, the Finsler metric function F is usually written in terms of the canonical coordinates of the tangent bundle

$(x, y) = (x^I, y^I)$, where $y = y^I \frac{\partial}{\partial x^I}$ is any tangent vector y at x. Then the Finsler metric tensor $\hat{g}_{IJ}$ is defined as

$$\hat{g}_{IJ}(x, y) = \frac{1}{2} \frac{\partial^2 F^2(x, y)}{\partial y^I \partial y^J}, \tag{13}$$

thus allowing us to write Eq. (11) as $d\hat{s}^2 = \hat{g}_{IJ}(x, y) y^I y^J$. Riemann spaces are particular cases of Finsler spaces, corresponding to $\hat{g}_{IJ}(x, y) = g_{IJ}(x)$, $y^I = dx^I$, and $ds^2 = g_{IJ}(x)dx^I dx^J$, respectively.

Another important geometric quantity, the Cartan tensor $\hat{C}(x, y)$, is defined according to

$$\hat{C}_{IJK} = \frac{1}{2} \frac{\partial \hat{g}_{IJ}(x, y)}{\partial y^K}. \tag{14}$$

2.1.1 Randers, Kropina and general (α, β) metrics

The Randers space, which has many applications in physics, is a special kind of Finsler space [9], with the Finsler metric function given by

$$F = \left[g_{IJ}(x)dx^I dx^J \right]^{1/2} + A_I(x)dx^I = \alpha + \beta, \tag{15}$$

where $g_{IJ}(x)$ is the fundamental tensor (metric) of a *Riemannian space*, and $A_I(x)dx^I$ is a linear one-form on the tangent bundle TM. Kropina [101,102] considered Finsler spaces with metrics given by

$$F(x, y) = \frac{g_{IJ}(x)y^I y^J}{A_I(x)y^I}. \tag{16}$$

These early results were generalized by Matsumoto [107, 108], who introduced *the notion of the (α, β) metrics*. A Finsler metric function $F(x, y)$ is called an (α, β) metric when F is a positively homogeneous function $F(\alpha, \beta)$ of the first degree in two variables $\alpha(x, y) = \left[g_{IJ}(x)dx^I dx^J \right]^{1/2}$ and $\beta(x, y) = A_I(x)y^I$, respectively.

In the following we will assume that α is *a Riemannian metric*; that is, it has the basic properties of being non-degenerate (regular) and positive-definite. The Randers and the Kropina metrics belong to the class of (α, β) metrics, with $F = \alpha + \beta$ for the case of the Randers metric and $F = \frac{\alpha^2}{\beta}$ for the case of the Kropina metric. Moreover, we can introduce general (α, β) metrics having the form

$$F(\alpha, \beta) = \alpha \phi \left(\frac{\beta}{\alpha} \right) = \alpha \phi(s), \tag{17}$$

where $s = \beta/\alpha$, and $\phi = \phi(s)$ is a C^∞ positive function on an open interval $(-b_o, b_o)$.

Denoting $L = F^2/2$, we obtain for the fundamental metric tensor of the (α, β) space the expression

$$\begin{aligned}
\hat{g}_{IJ}(x, y) &= \frac{L_\alpha}{\alpha} h_{IJ} + \frac{L_{\alpha\alpha}}{\alpha^2} y_I y_J + \frac{L_{\alpha\beta}}{\alpha} (y_I A_J + y_J A_I) \\
&\quad + L_{\beta\beta} A_I A_J,
\end{aligned} \tag{18}$$

where

$$h_{IJ} = \alpha \frac{\partial^2 \alpha(x, y)}{\partial y^I \partial y^J} = g_{IJ} - \frac{y_I y_J}{\alpha^2}, \tag{19}$$

and the indices α, β of L indicate partial differentiation with respect to α and β. Alternatively, one can compute the components of the Finslerian metric tensor by using the formula obtained in [109]. Let $\alpha = \sqrt{\epsilon g_{IJ}(x)y^I y^J}$, $\beta = A_I(x)y^I$, where $\epsilon = \pm 1$, and F is given by Eq. (17). Then the Hessian $\hat{g}$ can be obtained as

$$\hat{g}_{IJ} = \epsilon \rho g_{IJ} + \rho_0 b_I b_J + \rho_1 (b_I \alpha_J + b_J \alpha_I) - s\rho_1 \alpha_I \alpha_J, \tag{20}$$

where $\alpha_I := \alpha_{y^I}$ and

$$\rho = \phi^2 - s\phi\phi', \tag{21}$$
$$\rho_0 = \phi\phi'' + \phi'\phi', \tag{22}$$
$$\rho_1 = -s(\phi\phi'' + \phi'\phi') + \phi\phi'. \tag{23}$$

2.2 The Barthel connection and the osculating Finsler spaces

In the following we will briefly review the fundamental mathematical concepts on which the gravitational applications of the Kropina geometries are based, namely, the Barthel connection and the osculation of Finsler spaces.

2.2.1 The Barthel connection

Let us now assume that (M, F) is a Finsler space and $Y(x) \neq 0$ is a vector field defined on M. We can now introduce a specific structure $(M^n, F(x, y), Y(x))$ representing a Finsler space $(M^n, F(x, y))$ *having a tangent vector field $Y(x)$. If Y is nowhere vanishing, the Finslerian metric $\hat{g}(x, y)$ gives rise to the Y-Riemann metric $\hat{g}_Y(x) = \hat{g}(x, Y)$.*

An important class of Finsler spaces is the point Finsler spaces. Based on the definition introduced by Barthel [103, 104], *we consider in the following a Finsler space as an n-dimensional point space, which is locally Minkowskian and, in general, not locally Euclidean. A general Finsler space is both inhomogeneous and anisotropic, while a Minkowski space is flat and homogeneous, but anisotropic. Accordingly, we shall call the Finsler n-space a Barthel-Finsler space or, for short, a point Finsler space.*

Given a point vector field $Y^I(x)$ and a Finsler metric tensor $\hat{g}(x, y)$, one can construct the absolute differential of Y

according to the definition [110]

$$DY^I = dY^I + Y^K b^I_{KH}(x, Y) dx^H, \qquad (24)$$

where $b^I_{KH}(x, Y)$ are *the Barthel connection coefficients*. The Barthel connection coefficients are constructed with the help of the generalized Christoffel symbols $\hat{\gamma}_{JIH}$, defined as

$$\hat{\gamma}_{JIH} := \frac{1}{2}\left(\frac{\partial \hat{g}_{JI}}{\partial x^H} + \frac{\partial \hat{g}_{IH}}{\partial x^J} - \frac{\partial \hat{g}_{HJ}}{\partial x^I}\right), \qquad (25)$$

by writing the expressions in the second term of Eq. (24) as

$$Y^K b^I_{KH} = Y^K\left(\hat{\gamma}^I_{KH} - \hat{\gamma}^R_{KS} Y^S \hat{C}^I_{RH}\right), \qquad (26)$$

and defining the Barthel connection as [110]

$$b^I_{KH} = \hat{\gamma}^I_{KH} - \hat{\gamma}^R_{KS} Y^S \hat{C}^I_{RH}. \qquad (27)$$

The Barthel connection *depends on the field to which it is applied*, leading to a situation that is very different from the properties of the connection in Riemannian geometry. For anisotropic metrics, all properties can depend on the direction, and *in the case of the Barthel connection, the dependence is only on the direction of the field, and not on its magnitude*. The Barthel connection *is the simplest one that preserves the metric function by the parallel transport*. Moreover, for Finsler vector fields, depending on both x and y, it allows a natural passage to the standard Cartan geometry of Finsler spaces. Therefore, we can consider the Barthel connection *as the connection of a point Finsler space*.

From the general theory of the Finsler connections [5,6] it follows that these connections, unlike the usual Levi–Civita connection of a Riemannian metric, or more general affine connections, do not live on the base manifold M but on the total space of the tangent bundle. This essential difference sometimes induces major dissimilarities in the geometric theory of Riemannian and Finsler manifolds.

To fill in this gap, one of the possibilities is to evaluate the Finsler connections on a nowhere-vanishing tangent vector field $(x, Y(x))$, provided the topology of the base manifold M allows the existence of such vector fields. By evaluating the fundamental tensor $g_{ij}(x, y)$ of (M, F) at $(x, Y(x))$, one obtains a Riemannian metric g_Y on M, with its own Levi–Civita connection. Likewise, by evaluating the Cartan connection of (M, F) at $(x, Y(x))$ one obtains an affine connection on M, in general different from the Levi–Civita connection of g_Y, which is the Barthel connection already introduced above. Barthel himself arrived at this connection when studying the parallel transport on M.

2.2.2 The osculating Riemannian metric

In this subsection we will introduce the osculating Riemannian metric associated with a Finsler metric (M, F). The concept of osculating Riemannian spaces of Finsler spaces was introduced by Nazim [111], and it was later studied extensively in [112]. In simple terms, the osculation means that a rather complicated structure (Finsler geometry, Finsler connection) has an associated simpler structure (a Riemannian metric, an affine, or linear connection), with the simpler structure assumed to approximate the former in some sense. Based on this link, one can obtain results on the more complicated structure.

If we fix such a local section Y of $\pi_M : TM \to M$, all geometric objects defined on the manifold TM can be pulled back to M. Since $\hat{g}_{IJ} \circ Y$ is a function on U, we can define

$$\hat{g}_{IJ}(x) := \hat{g}_{IJ}(x, y)|_{y=Y(x)}, \quad x \in U. \qquad (28)$$

The pair $(U, \hat{g}_{IJ})$ is a Riemannian manifold, while $\hat{g}_{IJ}(x)$ is called the *Y-osculating Riemannian metric* associated with (M, F).

For the osculating Riemannian metric (28), the Christoffel symbols of the first kind are defined according to

$$\hat{\gamma}_{IJK}(x) := \frac{1}{2}\left(\frac{\partial}{\partial x^J}\left[\hat{g}_{IK}(x, Y(x))\right] + \frac{\partial}{\partial x^K}\left[\hat{g}_{IJ}(x, Y(x))\right]\right.$$
$$\left. - \frac{\partial}{\partial x^I}\left[\hat{g}_{JK}(x, Y(x))\right]\right).$$

By using the derivative law of composed functions we obtain

$$\hat{\gamma}_{IJK}(x) = \hat{\gamma}_{IJK}(x, y)|_{y=Y(x)}$$
$$+ 2\left(\hat{C}_{IJL}\frac{\partial Y^L}{\partial x^K} + \hat{C}_{IKL}\frac{\partial Y^L}{\partial x^J} - \hat{C}_{JKL}\frac{\partial Y^L}{\partial x^I}\right)\Big|_{y=Y(x)}. \qquad (29)$$

In the case of a general (α, β) metric for the Cartan tensor, we obtain

$$2\hat{C}_{IJK} = \frac{L_{\alpha\beta}}{\alpha}(h_{IJ}p_K + h_{JK}p_I + h_{KI}p_J) + L_{\beta\beta\beta}p_I p_J p_K, \qquad (30)$$

respectively, where we have denoted

$$y_I = g_{IJ}y^J, \quad p_I = A_I - \frac{\beta}{\alpha^2}y_I. \qquad (31)$$

Hence, if Y is a nonvanishing global section of TM, so that $Y(x) \neq 0, \forall x \in M$, one can always define the osculating Riemannian manifold $(M, \hat{g}_{ij})$.

In the case of an (α, β) metric, let us consider the vector field $Y = A$, where $A^I = g^{IJ}A_J$. Since the vector field A is globally nonvanishing on M, it follows that β has no zero points. Hence, we can introduce *the A-osculating Riemannian manifold* $(M, \hat{g}_{IJ})$, where $\hat{g}_{IJ}(x) := \hat{g}_{IJ}(x, A)$.

Let $\tilde{a}$ be the length of A with respect to α. Hence,

$$\tilde{a}^2 = A_I A^I = \alpha^2(x, A), \quad Y_I(x, A) = A_I. \qquad (32)$$

Therefore, the A-osculating Riemannian metric becomes

$$
\begin{aligned}
\hat{g}_{IJ}(x) = \left. \frac{L_\alpha}{\tilde{a}} \right|_{y=A(x)} g_{IJ} \\
+ \left(\frac{L_{\alpha\alpha}}{\tilde{a}^2} + 2\frac{L_{\alpha\beta}}{\tilde{a}} + L_{\beta\beta} - \frac{L_\alpha}{\tilde{a}^3} \right)\Bigg|_{y=A(x)} A_I A_J.
\end{aligned}
\tag{33}
$$

Moreover, we have

$$
\beta(x, A) = \tilde{a}^2, \quad p_I(x, A) = 0,
\tag{34}
$$

and consequently from Eq. (30) we obtain the important result that $\hat{C}_{IJK}(x, A) = 0$. On other hand, for $Y = A$, we obtain

$$
\hat{\gamma}_{IJK}(x) = \hat{\gamma}_{IJK}(x, y)\big|_{y=A(x)}.
\tag{35}
$$

Hence, for *a Finsler space with (α, β)-metric the linear A-connection with $A^I = (g^{IJ}A_J)$ (the Barthel connection), is the Levi–Civita connection of the A-Riemannian metric.*

2.3 The curvature tensor and its contractions

The curvature tensor of an affine connection with local coefficients $\left(\Gamma^A_{BC}(x)\right)$ is given by

$$
R^A_{BCD} = \frac{\partial \Gamma^A_{BD}}{\partial x^C} - \frac{\partial \Gamma^A_{BC}}{\partial x^D} + \Gamma^E_{BD}\Gamma^A_{EC} - \Gamma^E_{BC}\Gamma^A_{ED},
\tag{36}
$$

The Barthel connection with local coefficients $\left(b^A_{BC}(x)\right)$ *is an affine connection, and hence its curvature tensor must be given by the above formula*, with $\left(\Gamma^A_{BC}(x)\right) = \left(b^A_{BC}(x)\right)$. As we have already mentioned, in the case of the Kropina metric $F = \alpha^2/\beta$, the Barthel connection coincides with the Levi–Civita connection of the osculating metric $\hat{g}_{AB}(x) = g_{AB}(x, A(x))$, where $A_I(x)$ are the components of β, and g_{AB} is the fundamental tensor of F. Hence, since $b^A_{BC} = \hat{\gamma}^A_{BC}$, where $\hat{\gamma}^A_{BC}$ are the Levi–Civita coefficients, we obtain for the curvature tensors the expressions

$$
\hat{R}^A_{BCD} = \frac{\partial \hat{\gamma}^A_{BD}}{\partial x^C} - \frac{\partial \hat{\gamma}^A_{BC}}{\partial x^D} + \hat{\gamma}^E_{BD}\hat{\gamma}^A_{EC} - \hat{\gamma}^E_{BC}\hat{\gamma}^A_{ED},
\tag{37}
$$

and

$$
\hat{R}_{BD} = \sum_A \left[\frac{\partial \hat{\gamma}^A_{BD}}{\partial x^A} - \frac{\partial \hat{\gamma}^A_{BA}}{\partial x^D} + \sum_E \left(\hat{\gamma}^E_{BD}\hat{\gamma}^A_{EA} - \hat{\gamma}^E_{BA}\hat{\gamma}^A_{ED} \right) \right],
\tag{38}
$$

respectively, where $A, B, C, D, E \in \{0, 1, 2, 3\}$. For further details on the definitions of the affine connections and the curvature tensors, see [100] and references therein.

The contractions of the curvature tensor lead to the generalized Ricci tensor and Ricci scalar, respectively given by

$$
\hat{R}_{BD} = \hat{R}^A_{BAD}, \quad \hat{R}^B_D = \hat{g}^{BC}\hat{R}_{CD},
\tag{39}
$$

and

$$
\hat{R} = \hat{R}^B_B,
\tag{40}
$$

respectively.

3 Cosmological evolution in Barthel–Kropina geometry

In the present section, we will consider the general framework of the cosmological evolution in a Barthel–Kropina type geometry. We will begin by formulating a theoretical framework for the geometric and physical quantities of our model, in which the geometric and physical quantities are defined. As a next step, we will consider the computation of the geometric quantities (metric, Christoffel symbols and curvatures) in the adopted geometry. Finally, the generalized Friedmann equations describing the cosmological evolution are obtained.

3.1 Metric and thermodynamic quantities

In order to systematically construct the cosmology of the Barthel–Kropina geometry, and to facilitate the physical interpretation of the results, we adopt the following assumptions.

The Riemannian metric $g_{IJ}(x)$ in α is given by the Friedmann–Lemaître–Robertson–Walker (FLRW) metric,

$$
ds^2 = \left(dx^0\right)^2 - a^2\left(x^0\right)\left[\left(dx^1\right)^2 + \left(dx^2\right)^2 + \left(dx^3\right)^2 \right],
\tag{41}
$$

where we have adopted a coordinate system with $(x^0 = ct, x^1 = x, x^2 = y, x^3 = z)$, and $a\left(x^0\right)$ is the cosmological scale factor. The FLRW metric describes a homogeneous and isotropic universe, in which the cosmological time t is flowing uniformly.

The Barthel–Kropina metric components are functions of x^0 only. We adopt the *cosmological principle*, which requires that *the global and large-scale physical and geometric properties of the universe depend on the cosmological time only.* The cosmological principle requires that the components of the vector A in the one-form β are functions of the cosmological time only, $A_I = A_I\left(x^0\right)$.

The space-like components of A vanish. The cosmological principle, together with the diagonal nature of the FLRW metric, imposes another mathematical condition on the one-form β. More exactly, we require that the space-like components of A vanish so that $A_1 = A_2 = A_3 = 0$. If this condition were not satisfied, we could perform a spatial rotation, thus obtaining a preferred direction, for example, in the x coordinates. But such a cosmological model would contradict the observationally well-confirmed, large-scale spatial isotropy of the universe. Therefore, we assume that *the vector A has only one time-like independent component, $A_0\left(x^0\right)$*. Hence,

we represent the one-form field β as

$$(A_I) = \left(a\left(x^0\right)\eta\left(x^0\right), 0, 0, 0\right) = \left(A^I\right), \qquad (42)$$

where $\eta\left(x^0\right)$ is an arbitrary function of time to be determined from the gravitational field equations.

A frame comoving with matter does exist. Similarly to the standard general relativistic case and its Riemannian geometry, we assume that in the Barthel–Kropina geometry one can introduce a *comoving frame*, in which the motion of all observers take place with the Hubble flow, defined by the Riemannian metric $g_{IJ}(x)$.

Thermodynamic properties. We assume that the thermodynamic properties of the cosmological matter can be described by *two physical quantities only, the energy density ρc^2 and the thermodynamic pressure p*, respectively, defined in the standard way. From assumptions c and d it follows that the only nonvanishing components of the matter energy–momentum tensor $\hat{T}_{AB}$ are $\hat{T}_0^0 = \rho c^2$, $\hat{T}_{00} = \hat{g}_{00}\hat{T}_0^0$ and $\hat{T}_k^k = -p$, $\hat{T}_{ii} = -\hat{g}_{ik}\hat{T}_i^k$, respectively.

The gravitational field equations We postulate that the Einstein gravitational field equations can be formulated in a Barthel–Kropina geometry as

$$\hat{R}_{BD} - \frac{1}{2}\hat{g}_{BD}\hat{R} = \kappa^2 \hat{T}_{BD}, \qquad (43)$$

where $\kappa^2 = 8\pi G/c^4$ is a constant, and G and c are the Newtonian gravitational constant and the speed of light, respectively. $\hat{T}_{BD}$ is the matter energy–momentum tensor, *constructed with the help of the usual thermodynamic quantities as defined in the standard Riemann geometry, and of the Finslerian metric tensor $\hat{g}_{BD}$.*

In the present investigation, we have adopted for the Einstein equations (43) the simplest possible mathematical form, guided by the analogy with standard general relativity. Moreover, the adopted field equations have a well-defined Riemannian limit, corresponding to the case $\hat{g}(x, y) \rightarrow g(x)$, when we directly recover standard general relativity, without the cosmological constant term. There are many extensions of general relativity, and other forms of the field equations, inspired by these extensions, are also possible. For example, in the $f(R)$ modified gravity theory, introduced in [113], the gravitational Lagrangian is an arbitrary function of the Ricci scalar R. One could assume in the framework of a Finsler variational principle that the field equations follow from a Finsler type Lagrangian of the form $f\left(\hat{R}\right)$. Alternatively, one could construct the field equations in a less rigorous approach directly by substituting in the standard general relativistic equations the Riemannian quantities with their Finslerian counterparts. Modified gravity theories with curvature–matter coupling [114–116] could also be extended to a Finslerian geometric framework. Riemannian geometries with torsion [117,118] or non-metricity [119–121] can also represent a source of inspiration for obtaining their Finslerian analogues.

Hence, based on the above assumptions, the metric properties of Barthel–Kropina-FLRW model are given by

(i) $\epsilon = 1$;
(ii) $(A_I) = \left(a\left(x^0\right)\eta\left(x^0\right), 0, 0, 0\right) = \left(A^I\right)$;
(iii) $(g_{IJ}) = \begin{pmatrix} 1 & 0 & 0 & 0 \\ 0 & -a^2(x^0) & 0 & 0 \\ 0 & 0 & -a^2(x^0) & 0 \\ 0 & 0 & 0 & -a^2(x^0) \end{pmatrix}$;
(iv) $\alpha|_{y=A(x)} = a(x^0)\eta(x^0)$;
(v) $\beta|_{y=A(x)} = [a(x^0)\eta(x^0)]^2$;

3.2 Geometric quantities in Barthel–Kropina-FLRW geometry

As a first step in constructing a geometric theory in the Barthel–Kropina geometry, we need to obtain the components of the Finslerian metric tensor (the Hessian), which are given by (for the full computational details see Appendix A)

$$\hat{g}_{IJ}(x, A) = \frac{1}{\alpha^2}\left(2\epsilon g_{IJ} - \frac{A_I A_J}{\alpha^2}\right). \qquad (44)$$

Next, we need to obtain the Barthel–Kropina-FLRW Finsler metric, using the geometric properties introduced in the previous section. We immediately obtain

$$\hat{g}_{00} = \frac{1}{\alpha^2}\left(2g_{00} - \frac{A_0^2}{\alpha^2}\right) = \frac{1}{a^2\eta^2}\left[2 - \frac{(a\eta)^2}{(a\eta)^2}\right]$$
$$= \frac{1}{a^2\eta^2}. \qquad (45)$$

For $i, j \in \{1, 2, 3\}$ we find

$$\hat{g}_{ij} = \frac{1}{\alpha^2}\left(2g_{ij} - \frac{A_i A_j}{\alpha^2}\right) = \frac{1}{\alpha^2}\left(2g_{ii} - \frac{A_i^2}{\alpha^2}\right)\delta_{ij}$$
$$= \frac{1}{a^2\eta^2}\left[2(-a^2)\right]\delta_{ij} = -\frac{2}{\eta^2}\delta_{ij}. \qquad (46)$$

Hence, we obtain the nonvanishing components of the Barthel–Kropina-FLRW metric tensor $\hat{g}_{IJ}$ as given by

$$\hat{g}_{IJ} = \begin{cases} \hat{g}_{00} = \dfrac{1}{a^2(x^0)\eta^2(x^0)}, \\[2mm] \hat{g}_{ij} = \dfrac{-2}{\eta^2(x^0)}\delta_{ij}, i, j = 1, 2, 3. \end{cases}$$

The inverse components of the Barthel–Kropina-FLRW metric tensor $\hat{g}_{IJ}$ can be obtained as

$$\hat{g}^{IJ} = \begin{pmatrix} a^2\eta^2 & 0 & 0 & 0 \\ 0 & -\dfrac{\eta^2}{2} & 0 & 0 \\ 0 & 0 & -\dfrac{\eta^2}{2} & 0 \\ 0 & 0 & 0 & -\dfrac{\eta^2}{2} \end{pmatrix}.$$

For the Christoffel symbols associated with the Barthel–Kropina-FLRW metric, we obtain (the detailed calculations are presented in Appendix B)

$$\hat{\gamma}^0_{00} = -\frac{(\eta\mathcal{H} + \eta')}{\eta}, \ \hat{\gamma}^0_{ij} = -\frac{-2a^2\eta'}{\eta}\delta_{ij}, \ \hat{\gamma}^i_{0j} = -\frac{\eta'}{\eta}\delta^i_j,$$

where $\mathcal{H} = \frac{a'}{a}$.

The nonvanishing components of the Ricci tensor are given by (see Appendix C for the calculational details)

$$\hat{R}_{00} = \frac{3}{\eta^2}\left[\eta\eta'' + \eta\eta'\mathcal{H} - (\eta')^2\right], \tag{47}$$

and

$$\hat{R}_{ij} = \frac{2a^2}{\eta^2}\left(3(\eta')^2 + \eta\eta'' + \eta\eta'\mathcal{H}\right)\delta_{ij}, \tag{48}$$

respectively. For the Ricci scalar $\hat{R} = \hat{g}^{IJ}\hat{R}_{IJ}$ we find (see Appendix D)

$$\hat{R} = 6a^2(\eta\eta'' + \mathcal{H}\eta\eta' - 2(\eta')^2). \tag{49}$$

Finally, we obtain the Einstein tensor components

$$\hat{G}_{IJ} = \hat{R}_{IJ} - \frac{1}{2}\hat{R}\hat{g}_{IJ},$$

as

$$\hat{G}_{00} = \hat{R}_{00} - \frac{1}{2}\hat{R}\hat{g}_{00} = \frac{3(\eta')^2}{\eta^2}, \tag{50}$$

and

$$\hat{G}_{ij} = \hat{R}_{ij} - \frac{1}{2}\hat{R}\hat{g}_{ij}$$
$$= \frac{2a^2}{\eta^2}\left[-3(\eta')^2 + 2\eta\eta'' + 2\mathcal{H}\eta\eta'\right]\delta_{ij}, \tag{51}$$

respectively. For the explicit calculations of these components see Appendix E.

3.3 The generalized Friedmann equations

Once the geometric quantities in the Barthel–Kropina-FLRW geometry are known, we can write the full set of Einstein gravitational field equations relating geometry and matter. By taking into account our assumptions about the physical nature of the cosmological quantities, the Einstein field equations

$\hat{G}_{00} = (8\pi G/c^4)\,\hat{g}_{00}\rho$ and $\hat{G}_{ii} = -(8\pi G/c^4)\,\hat{g}_{ii}\,p$ lead to the system of the generalized Friedmann equations, given by

$$\frac{3(\eta')^2}{\eta^2} = \frac{8\pi G}{c^2}\frac{1}{a^2\eta^2}\rho, \tag{52}$$

and

$$a^2\left[-3(\eta')^2 + 2\eta\eta'' + 2\mathcal{H}\eta\eta'\right] = \frac{8\pi G}{c^4}p, \tag{53}$$

respectively. By replacing the term $-3(\eta')^2$ with the help of Eq. (52), Eq. (53) takes the alternative form

$$2a\eta\frac{d}{dx^0}(\eta'a) = \frac{8\pi G}{c^4}\left(\rho c^2 + p\right). \tag{54}$$

3.4 General relativistic limit and the energy balance equation

A first interesting property of the cosmological equations of the Barthel–Kropina-FLRW model is that *in the limit $\eta \rightarrow \pm 1/a$, $\beta = (1, 0, 0, 0)$, the generalized Friedmann Eqs.* (52) *and* (53) *do reduce to the standard Friedmann equations of general relativity,*

$$\frac{3(a')^2}{a^2} = \frac{8\pi G}{c^2}\rho, \tag{55}$$

$$2\frac{\ddot{a}}{a} + \frac{(a')^2}{a^2} = -\frac{8\pi G}{c^4}p, \tag{56}$$

a result which is easy to check. From the Friedmann equations of standard general relativistic cosmology, it follows that the matter energy density ρ satisfies the conservation equation

$$\dot{\rho} + 3H\left(\rho + \frac{p}{c^2}\right) = 0, \tag{57}$$

where the dot denotes the derivative with respect to the time, and $H = c\mathcal{H}$. For $p = 0$, the conservation equation can be immediately integrated to give

$$\rho = \frac{\rho_0}{a^3} = \rho_0(1 + z)^3, \tag{58}$$

where $\rho_0 = \rho_{0b} + \rho_{0DM}$ is the present-day matter density of the universe, with ρ_{0b} and ρ_{0DM} denoting the present-day density of the baryonic and dark matter, respectively, and we have introduced the redshift variable, defined as $1/z = 1+a$. We now introduce the generalized matter density parameter Ω_m, defined as

$$\Omega_m = \frac{\rho}{\rho_0} = \frac{1}{a^3} = (1 + z)^3. \tag{59}$$

By considering a three-component universe filled with ordinary matter, dark matter, and dark energy, respectively, in the standard ΛCDM model, the Hubble function is given by

$$H = H_0\sqrt{\frac{\Omega_m^{(cr)}}{a^3} + \Omega_\Lambda} = H_0\sqrt{\Omega_m^{(cr)}(1 + z)^3 + \Omega_\Lambda}, \tag{60}$$

where $\Omega_m^{(cr)} = \Omega_b^{(cr)} + \Omega_{DM}^{(cr)}$, and $\Omega_b^{(cr)} = \rho_b/\rho_{cr}$, $\Omega_{DM} = \rho_{DM}/\rho_{cr}$ and $\Omega_\Lambda = \Lambda/\rho_{cr}$ denote the density parameters of the baryonic matter, dark matter, and dark energy, respectively. Here, ρ_{cr} denotes the critical density of the universe, defined as $\rho_{cr} = 3H_0^2/8\pi G$. An important observational parameter, the deceleration parameter is defined as

$$q = \frac{d}{dt}\frac{1}{H} - 1. \tag{61}$$

In the ΛCDM model, the deceleration parameter is obtained as

$$q(z) = \frac{3(1+z)^3\Omega_m}{2\left[\Omega_\Lambda + (1+z)^3\Omega_m\right]} - 1. \tag{62}$$

To compare the predictions of the Barthel–Kropina-FLRW cosmological model with observations and with the ΛCDM model, we adopt for the matter and dark energy density parameters the values $\Omega_{DM} = 0.2589$, $\Omega_b = 0.0486$, and $\Omega_\Lambda = 0.6911$, respectively [22]. Then, for the total matter density parameter $\Omega_m = \Omega_{DM} + \Omega_b$, we obtain $\Omega_m = 0.3089$. The present-day value of the deceleration parameter has the value $q(0) = -0.5381$, indicating that at present the universe is in an accelerating phase.

3.4.1 The Riemannian limit of the Kropina metric

We now consider the limiting case of the Finsler metric. Since in the case of the considered Kropina metric, $F = \alpha^2/\beta$, with $\alpha^2 = g_{IJ}(x)dy^I dy^j$ and $\beta = A_I dy^I$, the standard general relativistic Riemann geometry is recovered in the limit $\beta \to \alpha$, which gives $\lim_{\beta\to\alpha} F = \alpha = \sqrt{g_{IJ}(x)y^I y^J}$. The condition $\alpha = \beta$ gives immediately $g_{IJ}y^I y^J = A_I A_J y^I y^J$, or $\lim_{\alpha\to\beta} \hat{g}_{IJ} = A_I A_J$. This means that the limiting Riemann metric g_{IJ} is actually an inner product, and hence it becomes a degenerate Riemann metric in the sense that $\det|g_{IJ}| = 0$; that is, $\mathrm{rank}\, g_{IJ} = n - 1$.

Equivalently, by taking the limit $\beta \to \alpha$ in Eq. (A1), giving the metric tensor of the Barthel–Kropina geometry, one can show that $\lim_{\beta\to\alpha} \hat{g}_{IJ} = g_{IJ} = A_I A_J$. The fact that in the Riemannian limit the Kropina metric leads to a degenerate Riemann metric should not come as a surprise. Indeed, the original Kropina metric is degenerate at the origin of $T_x M$, and by taking the limit $\beta \to \alpha$, we obtain a degenerate Riemann metric.

This also means that in this limit, the Kropina indicatrix degenerates into the Riemannian unit circle of the degenerate metric g_{IJ}. Since $\lim_{\beta\to\alpha} \hat{g}(x, y) = g_{IJ}(x)$, under the same limit the Y-osculating metric $\hat{g}(x, Y(x)) = \hat{g}(x)$ tends to $g_{IJ}(x)$, which is degenerate, as already explained. Moreover, let us observe that the condition $g_{IJ} \to A_I A_J$ is incompatible with the choice $g_{IJ} = \mathrm{diag}\left(1, -a^2, -a^2, -a^2\right)$ and $b_I = (b_0, 0, 0, 0)$, respectively, except for the case $a^2 = 0$, which is obviously meaningless in the present context.

3.4.2 The energy balance equation

We now multiply Eq. (52) by a^3, and take the derivative of the resulting relation with respect to x^0. Thus, we obtain

$$\frac{8\pi G}{c^2}\frac{d}{dx^0}\left(\rho a^3\right) = 15a^4 a'\left(\eta'\right)^2 + 6a^5\eta'\eta''. \tag{63}$$

After multiplying Eq. (53) by $3a^2 a'$, we obtain

$$\frac{8\pi G}{c^4}p\frac{d}{dx^0}a^3 = -9a^4 a'\left(\eta'\right)^2 + 6a^4 a'\eta\eta'' + 6a^4 a'\mathcal{H}\eta\eta'. \tag{64}$$

By adding Eqs. (63) and (64), we obtain the energy balance equation in the Barthel–Kropina-FLRW cosmological model as

$$\frac{8\pi G}{c^4}\left[\frac{d}{dx^0}\left(\rho c^2 a^3\right) + p\frac{d}{dx^0}a^3\right] = 6a^5\Big[\mathcal{H}\left(\eta'\right)^2 + \left(\eta' + \mathcal{H}\eta\right)\eta'' + \mathcal{H}^2\eta\eta'\Big]. \tag{65}$$

The energy balance equation can be reformulated, using the generalized Friedmann equations, as

$$\frac{8\pi G}{c^4}\left[\frac{d}{dx^0}\left(\rho c^2 a^3\right) + p\frac{d}{dx^0}a^3\right]$$
$$= 6a^5\left[\frac{8\pi G}{2c^4}\left(\frac{5}{3}\rho c^2 + p\right)\frac{\mathcal{H}}{a^2} + \eta'\eta''\right]. \tag{66}$$

4 Particular cosmological models

In the present section, we will investigate the cosmological implications of the generalized Friedmann equations (52) and (53) obtained within the framework of the Barthel–Kropina-FLRW geometry.

4.1 The de Sitter solution

The de Sitter solution corresponds to an exponential expansion in the Riemann geometric framework, with $a\left(x^0\right) = e^{\mathcal{H}_0 x^0}$, where $\mathcal{H}_0 = \mathcal{H} = \text{constant}$. The system of the generalized Friedmann equations does not admit an explicit vacuum solution, since $\rho = p = 0$ implies $\eta' = 0$, $\eta = \text{constant}$, and the second Friedmann equation (53) is automatically satisfied. Hence, a de Sitter type exponential expansion can take place only in the presence of matter. Thus, we assume a nonzero matter energy density, but a vanishing thermodynamic pressure for the cosmological matter, with $p = 0$. In the case $\mathcal{H} = \mathcal{H}_0 = \text{constant}$, Eq. (53) becomes

$$-3(\eta')^2 + 2\eta\eta'' + 2\mathcal{H}_0\eta\eta' = 0. \tag{67}$$

By introducing a new variable u, defined as $\eta' = u$, we immediately obtain $\eta'' = du/dx^0 = (du/d\eta)(d\eta/dx^0) =$

$u(du/d\eta)$. Hence, Eq, (67) becomes

$$\frac{du}{d\eta} = \frac{3}{2}\frac{u}{\eta} - \mathcal{H}_0, \tag{68}$$

with the general solution given by

$$u(\eta) = C_1 \eta^{3/2} + 2\mathcal{H}_0 \eta, \tag{69}$$

where C_1 is an arbitrary constant of integration. Therefore, from

$$\frac{d\eta}{dx^0} = C_1 \eta^{3/2} + 2\mathcal{H}_0 \eta, \tag{70}$$

we obtain the general solution of Eq. (67) as

$$\eta\left(x^0\right) = \frac{4\mathcal{H}_0^2 e^{2\mathcal{H}_0(x^0+C_2)}}{\left[1 \pm C_1 e^{\mathcal{H}_0(x^0+C_2)}\right]^2}, \tag{71}$$

where C_2 is an integration constant that can be taken as zero without any loss of generality by a rescaling of the time coordinate x^0. Moreover, in order to obtain a physically consistent solution, we will adopt the minus sign in the above equation. Hence, a de Sitter type exponential expansion of the Riemann metric corresponds to

$$\eta\left(x^0\right) = \frac{4\mathcal{H}_0^2 e^{2\mathcal{H}_0 x^0}}{\left[1 - C_1 e^{\mathcal{H}_0 x^0}\right]^2}. \tag{72}$$

During the de Sitter phase, the matter energy density varies as

$$\frac{8\pi G}{c^2}\rho\left(x^0\right) = \frac{192\mathcal{H}_0^6 e^{6\mathcal{H}_0 x^0}}{\left(1 - C_1 e^{\mathcal{H}_0 x^0}\right)^6}. \tag{73}$$

At the initial moment $x^0 = 0$, the matter energy density is

$$\frac{8\pi G}{c^2}\left.\rho\left(x^0\right)\right|_{x^0=0} = \frac{192\mathcal{H}_0^6}{(1 - C_1)^6}, \tag{74}$$

while for $x^0 \to \infty$, we obtain

$$\frac{8\pi G}{c^2}\lim_{x^0\to\infty}\rho\left(x^0\right) = \frac{192\mathcal{H}_0^6}{C_1^6}. \tag{75}$$

In order to obtain a monotonically decreasing matter energy density during the de Sitter phase satisfying the condition $\left.\rho\left(x^0\right)\right|_{x^0=0} > \lim_{x^0\to\infty}\rho\left(x^0\right)$, the integration constant C_1 must satisfy the condition $C_1 > 1/2$.

4.2 Conservative cosmological evolution

We will now consider conservative Barthel–Kropina-FLRW models, that is, models in which the matter conservation equation

$$\frac{d}{dx^0}\left(\rho c^2 a^3\right) + p\frac{d}{dx^0}a^3 = 0, \tag{76}$$

is identically satisfied. In this case, the system of generalized Friedmann equations reduces to the Friedmann equations (52) and (53), together with the constraint

$$\mathcal{H}\left(\eta'\right)^2 + \left(\eta' + \mathcal{H}\eta\right)\eta'' + \mathcal{H}^2\eta\eta' = 0. \tag{77}$$

4.2.1 Linear barotropic fluid cosmological models

As a first example of a conservative Barthel–Kropina-FLRW cosmological model, we consider the case of a barotropic fluid-dominated universe, with $p = (\gamma - 1)\rho c^2$, where $\gamma =$ constant and $1 \leq \gamma \leq 2$. In this case, Eq. (76) immediately gives

$$\rho\left(x^0\right) = \frac{\rho_0}{a^{3\gamma}\left(x^0\right)}, \tag{78}$$

where ρ_0 is an integration constant. Then, Eq. (52) gives

$$\eta' = -\sqrt{\frac{8\pi G\rho_0}{3c^2}}\frac{1}{a^{3\gamma/2+1}}, \tag{79}$$

$$\eta'' = \left(\frac{3\gamma}{2} + 1\right)\sqrt{\frac{8\pi G\rho_0}{3c^2}}\frac{a'}{a^{3\gamma/2+2}}, \tag{80}$$

where we have assumed that η is a monotonically decreasing function of time.

By taking into account the linear barotropic equation of state, using Eq. (52), the pressure can be obtained as

$$p = (\gamma - 1)\rho c^2 = 3(\gamma - 1)\frac{c^4}{8\pi G}a^2\left(\eta'\right)^2. \tag{81}$$

After substituting the above expression of the pressure in Eq. (53), we obtain the equation

$$2\eta\eta'' + 2\mathcal{H}\eta\eta' = 3\gamma\left(\eta'\right)^2, \tag{82}$$

which can be integrated immediately to obtain the first integral

$$\left|\eta'\right| a = C^{-3\gamma/2}\eta^{3\gamma/2}, \tag{83}$$

where C is an arbitrary integration constant. Using the expression (79) for η', we obtain

$$\eta(a) = C\left(\frac{8\pi G\rho_0}{3c^2}\right)^{1/3\gamma}a^{-1}. \tag{84}$$

By taking the derivative of the above expression of η with respect to x^0, and equating it with η' obtained from the first Friedmann equation as given by Eq. (79), we obtain for a' the equation

$$\frac{a'}{a^2} = \frac{1}{C}\left(\frac{8\pi G\rho_0}{3c^2}\right)^{(3\gamma-2)/6\gamma}\frac{1}{a^{3\gamma/2+1}}, \tag{85}$$

with the general solution given by $a\left(x^0\right) \propto \left(x^0\right)^{2/3\gamma}$. Hence, conservative Barthel–Kropina-FLRW cosmological models

exactly mimic their general relativistic counterparts, describing the decelerating evolution of a matter-dominated universe satisfying a linear barotropic equation of state. For a dust universe we obtain $a\left(x^0\right) = \left(x^0\right)^{2/3}$, while for a radiation-dominated universe, the scale factor varies as $a\left(x^0\right) = \left(x^0\right)^{1/2}$.

4.3 Nonconservative Barthel–Kropina-FLRW cosmological models

In the following we consider cosmological models in which the matter density and pressure do not satisfy the conservation Eq. (76), and thus for a linear barotropic equation of state, the expression of the energy density is different from the one given by Eq. (78). However, we will consider that matter still satisfies a linear barotropic equation of state. Hence, by eliminating the pressure from the second Friedmann equation (53) with the help of the equation of state and the first Friedmann equation (52), we obtain

$$\eta\eta'' + \mathcal{H}\eta\eta' = \frac{3\gamma}{2}\left(\eta'\right)^2,\tag{86}$$

which can be immediately integrated to give the first integral

$$|\eta'|\,a = C\eta^{3\gamma/2},\tag{87}$$

where C is an arbitrary constant of integration, and we have used the standard mathematical relation $\int\left(f'(x)/f(x)\right)\mathrm{d}x = \ln|f(x)|+C$. For the matter density we find the expression

$$\frac{8\pi G}{c^2}\rho = a^2\left(\eta'\right)^2 = C^2\eta^{3\gamma}.\tag{88}$$

In order to obtain a monotonically decreasing matter density, η must also be a decreasing function of time. In terms of η, the Hubble function is obtained as

$$\mathcal{H} = \frac{3\gamma}{2}\frac{\eta'}{\eta} - \frac{\eta''}{\eta'}.\tag{89}$$

Eqs. (87) and (88) give the full solution of the Friedmann equations for the cosmological evolution in the Barthel–Kropina-FLRW geometry. Once the functional form of η is specified, the evolution of the scale factor and the other cosmological parameters can be immediately obtained.

4.3.1 $\eta = \eta(a)$

As a first example of a nonconservative Barthel–Kropina-FLRW cosmological model, we consider the case in which η is a function of the scale factor only, $\eta = \eta(a)$. Then, Eq. (87) immediately gives the evolution equation

$$a\frac{\mathrm{d}\eta(a)}{\mathrm{d}a}a' = C\eta^{3\gamma/2}(a),\tag{90}$$

which can be integrated to give

$$C\left(x^0 - x_0^0\right) = \int a\frac{\mathrm{d}\eta(a)}{\mathrm{d}a}\eta^{-3\gamma/2}(a)\mathrm{d}a,\tag{91}$$

where x_0^0 is an arbitrary integration constant.

In the following we will consider the case of a dust universe with $\gamma = 1$. The simplest possible cosmological model can be obtained for $\eta(a) = a_1 a^{-n}$, where a_1 and n are constants. Then we immediately obtain

$$a\left(x^0\right) = \left(\frac{5\sqrt{a_1}C}{2}\right)^{2/(2-5n)}\left(x^0 - x_0^0\right)^{2/(2-5n)},\tag{92}$$

where we assume $5n < 2, n < 0.4$. For the Hubble function, we find

$$H\left(x^0\right) = \frac{2}{2 - 5n}\frac{1}{x^0},\tag{93}$$

while for the deceleration parameter we obtain the expression $q = -5n/2$. The universe is in an accelerated expansionary state, and the scale factor has a power law dependence on the time coordinate.

4.3.2 $\eta = \eta(\mathcal{H})$

As another particular class of Barthel–Kropina-FLRW cosmological models, we consider the case in which η is a function of $\mathcal{H}$, the Hubble function, so that $\eta = \eta(\mathcal{H})$. Hence, under this assumption, Eq. (87) takes the form

$$\frac{\mathrm{d}\eta(\mathcal{H})}{\mathrm{d}\mathcal{H}}\frac{\mathrm{d}\mathcal{H}}{\mathrm{d}x^0}a = C^{-3\gamma/2}\eta^{3\gamma/2}(\mathcal{H}).\tag{94}$$

At this moment we introduce as the independent variable the redshift z, defined as $1 + z = 1/a$. Hence, we obtain

$$\frac{d}{dx^0} = \frac{\mathrm{d}z}{\mathrm{d}x^0}\frac{d}{\mathrm{d}z} = -(1 + z)\mathcal{H}(z)\frac{d}{\mathrm{d}z}.\tag{95}$$

In the redshift variable, Eq. (94) becomes

$$-(1 + z)^2\frac{\mathrm{d}\eta(\mathcal{H}(z))}{\mathrm{d}\mathcal{H}(z)}\mathcal{H}(z)\frac{\mathrm{d}\mathcal{H}(z)}{\mathrm{d}z}$$
$$= C^{-3\gamma/2}\eta^{3\gamma/2}(\mathcal{H}(z)).\tag{96}$$

In the following we adopt for $\eta(\mathcal{H})$ the simple form

$$\eta(\mathcal{H}) = a_1\mathcal{H}^n + b_1,\tag{97}$$

where a_1, b_1, and n are constants. We also rescale the Hubble function according to $\mathcal{H} = (1/c)H = (1/c)H_0 h$, where H_0 is the present-day value of the Hubble function. Moreover, we rescale the coefficient a_1 as $a_1 \to a_1/H_0^n$. We consider the late-time evolution of the universe in its dust phase, with zero pressure, and therefore we take $\gamma = 1$. Hence, Eq. (96) takes the form

$$-(1 + z)^2 h^n(z)\frac{\mathrm{d}h(z)}{\mathrm{d}z} = c_1\left(a_1 h^n + b_1\right)^{3/2},\tag{98}$$
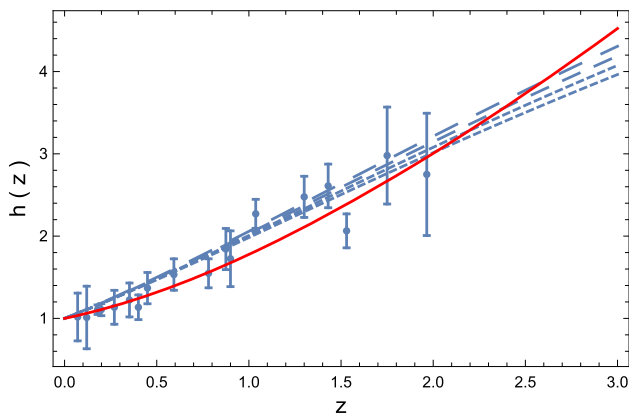
Fig. 1 Variation in the dimensionless Hubble function h as a function of the redshift z for $\eta(z) = a_1 h^n(z) + b_1$ for $n = 2/3$, $b_1 = -0.21$, $c_1 = 3.9$, and different values of a_1: $a_1 = 0.348$, (short dashed curve), $a_1 = 0.350$ (dashed curve), $a_1 = 0.352$, (long dashed curve), and $a_1 = 0.354$, (ultra-long dashed curve), respectively. The red solid line represents the prediction of the ΛCDM model. The observational data are represented together with their error bars

where we have denoted $c_1 = C^{-3/2}/na_1$. The matter energy density can be obtained as

$$\frac{8\pi G}{c^2}\rho = C^2 \left(a_1 \mathcal{H}^n + b_1\right)^3 . \tag{99}$$

For the matter density parameter, we obtain

$$\Omega_m = \frac{\rho}{\rho_0} = C_1 \left(a_1 h^n + b_1\right)^3 , \tag{100}$$

where we have denoted $C_1 = C^2 c^2 \rho_c / 3H_0^2 \rho_0$.

The variation in the normalized Hubble function, the deceleration parameter, and the matter density parameter are presented in Figs. 1, 2, and 3 for four values of n ($n = 1, 2, 3, 4$) and for different values of a_1, b_1, and c_1. In the figures we have also included the observational data for the Hubble function, together with their error bars [124,125], as well as the predictions of the ΛCDM model.

As one can see from Fig. 1, for the adopted functional form of η, the Barthel–Kropina-FLRW model gives an acceptable description of the observational data for $h(z)$, up to a redshift of around $z \approx 3$, and it can also reproduce, at least qualitatively, the predictions of the ΛCDM model. However, with increasing z, at redshifts higher than 3, important deviations from the predictions of the ΛCDM model do appear, with the dimensionless Hubble functions of the ΛCDM model increasing much faster than in Barthel–Kropina-FLRW cosmology.

For the adopted set of the model parameters, the comparison of the deceleration parameter curves, presented in Fig. 2, as predicted by the Barthel–Kropina-FLRW model and by the ΛCDM model indicate the existence of significant differences between the two models, especially at higher redshifts. Both models predict a late-time accelerating behavior, with
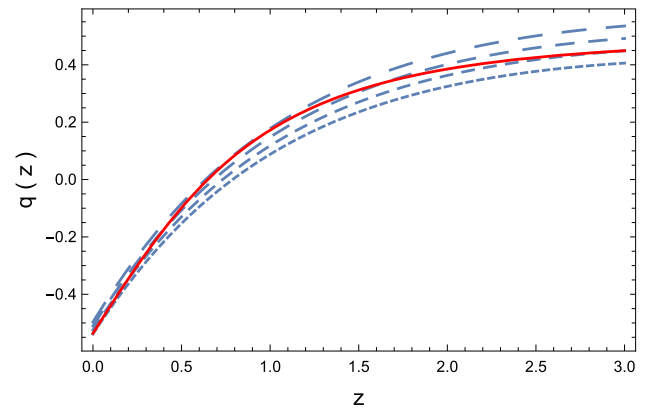
Fig. 2 Variation in the deceleration parameter q as a function of the redshift z for $\eta(z) = a_1 h^n(z) + b_1$ for $n = 2/3$, $b_1 = -0.21$, $c_1 = 3.9$, and different values of a_1: $a_1 = 0.348$, (short dashed curve), $a_1 = 0.350$ (dashed curve), $a_1 = 0.352$, (long dashed curve), and $a_1 = 0.354$, (ultra-long dashed curve), respectively. The red solid line represents the prediction of the ΛCDM model
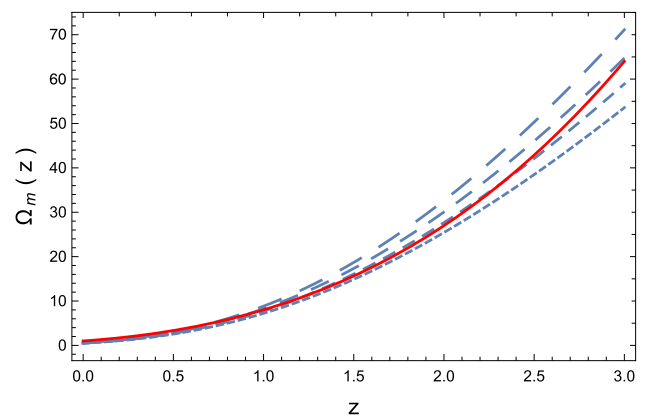
Fig. 3 Variation in the total matter density parameter Ω_m as a function of the redshift z for $\eta(z) = a_1 h^n(z) + b_1$ for $n = 2/3$, $b_1 = -0.21$, $c_1 = 3.9$, and different values of a_1: $a_1 = 0.348$, (short dashed curve), $a_1 = 0.350$ (dashed curve), $a_1 = 0.352$, (long dashed curve), and $a_1 = 0.354$, (ultra-long dashed curve), respectively. The red solid line represents the prediction of the ΛCDM model

$q < 0$ at the present time, but the numerical values for $q(0)$ differ considerably in the two models at redshifts $z > 0.5$. However, the present-day values of q in the Barthel–Kropina-FLRW cosmology are consistent with the predictions of the ΛCDM model. At larger redshifts, the behavior of the deceleration parameter q in the present Finsler type model strongly depends on the numerical values of the model parameters, and at redshifts higher than 3, significant deviations from the predictions of the ΛCDM model do occur.

At a qualitative level, the Barthel–Kropina-FLRW cosmology can also reproduce the behavior of the total matter density parameter Ω_m in the ΛCDM model. At low redshifts $0 \leq z < 1$, the predictions of the two models basically agree. However, the quantitative differences, already observed in the case of the deceleration parameter, do also exist for this

physical parameter. In the range $1 \leq z \leq 3$, the behavior of the matter density parameter strongly depends on the model parameters, ΛCDM, and at higher redshifts, both lower and higher matter density parameters can be obtained, thus leading to matter densities that are different from the predictions of the ΛCDM model.

5 Dark energy in the Barthel–Kropina-FLRW cosmology

We will now consider that the function η can be represented in a general form as

$$\eta = \frac{1}{a\left(x^0\right)}\left[1 + f\left(x^0\right)\right], \tag{101}$$

where f is an arbitrary function to be determined from the field equations. In the limit $f \to 0$, $\eta \to 1/a$, and as we have already seen, we recover the standard Friedmann equations of general relativity. With this representation of η, the generalized Friedmann equations take the form

$$3\frac{\left(a'\right)^2}{a^2} = \frac{8\pi G}{c^2}\rho + 6(1+f)\mathcal{H}f' - 3\left(f'\right)^2 - 3\mathcal{H}^2(2+f)f$$
$$= \frac{8\pi G}{c^2}\rho + \rho_{DE}, \tag{102}$$

and

$$\frac{2a''}{a} + \frac{\left(a'\right)^2}{a^2} = -\frac{8\pi G}{c^4}\frac{p}{(1+f)^2} + 4\mathcal{H}\frac{f'}{1+f} - 3\frac{\left(f'\right)^2}{(1+f)^2}$$
$$+ 2\frac{f''}{1+f}, \tag{103}$$

where

$$\rho_{DE} = 6(1+f)\mathcal{H}f' - 3\left(f'\right)^2 - 3\mathcal{H}^2(2+f)f, \tag{104}$$

and

$$p_{DE} = 4\mathcal{H}\frac{f'}{1+f} - 3\frac{\left(f'\right)^2}{(1+f)^2} + 2\frac{f''}{1+f}, \tag{105}$$

respectively. An effective dark energy term, satisfying the condition $p_{DE} = w\rho_{DE}$, $w = $ constant can be obtained if the function f satisfies the equation

$$\frac{2f''}{1+f} + 2\mathcal{H}\left[-3w(1+f) + \frac{2}{1+f}\right]f'$$
$$+ 3\left[w - \frac{1}{(1+f)^2}\right]\left(f'\right)^2 + 3wf(2+f)\mathcal{H}^2 = 0. \tag{106}$$

The dynamical cosmological dark energy is thus dependent on the scale factor and on the properties of η. In the following we will consider only the late-time evolution of the universe, and hence we take $p = 0$. To simplify the mathematical formalism, we introduce the dimensional time

parameter $\tau = \mathcal{H}_0 x^0$ and the normalized Hubble function h, defined as $\mathcal{H} = \mathcal{H}_0 h$, where $\mathcal{H}_0 = H_0/c$, and H_0 is the present-day value of the Hubble function. Moreover, we denote $u = df/d\tau$. Then the equations describing the cosmological dynamics of the Barthel–Kropina-FLRW cosmological model take the form

$$\frac{df}{d\tau} = u, \tag{107}$$

$$2\frac{dh}{d\tau} + 3h^2 = 4h\frac{u}{1+f} - 3\frac{u^2}{(1+f)^2} + \frac{2}{1+f}\frac{du}{d\tau}, \tag{108}$$

$$\frac{2}{1+f}\frac{du}{d\tau} + 2h\left[\frac{2}{1+f} - 3w(1+f)\right]u$$
$$+ 3\left[w - \frac{1}{(1+f)^2}\right]u^2 + 3wf(2+f)h^2 = 0. \tag{109}$$

By introducing the critical density $\rho_c = 3H_0^2/8\pi G$, and by defining the matter density parameter as $\Omega_m = \rho/\rho_c$, from the first Friedmann equation we obtain

$$\Omega_m = h^2 + \left(\frac{df}{d\tau}\right)^2 + (2+f)fh^2 - 2(1+f)h\frac{df}{d\tau}. \tag{110}$$

In terms of the redshift variable $1 + z = 1/a$, the system of equations (107)–(109) become

$$-(1+z)h\frac{df}{dz} = u, \tag{111}$$

$$-2(1+z)h\frac{dh}{dz} + 3h^2 = 4h\frac{u}{1+f} - 3\frac{u^2}{(1+f)^2}$$
$$-2(1+z)\frac{h}{1+f}\frac{du}{dz}, \tag{112}$$

$$-2(1+z)\frac{h}{1+f}\frac{du}{dz} + 2h\left[\frac{2}{1+f} - 3w(1+f)\right]u$$
$$+ 3\left[w - \frac{1}{(1+f)^2}\right]u^2 + 3wf(2+f)h^2 = 0. \tag{113}$$

For the redshift dependence of the matter density parameter, we find

$$\Omega_m = h^2\left[1 + (1+z)^2\left(\frac{df}{dz}\right)^2 + (2+f)f\right.$$
$$\left. + 2(1+z)(1+f)\frac{df}{dz}\right]. \tag{114}$$

For the deceleration parameter, we obtain

$$q = \frac{1}{2} + \frac{3}{2}\frac{\frac{8\pi G}{c^4}\frac{p}{(1+f)^2} - p_{DE}}{\frac{8\pi G}{c^2}\rho + \rho_{DE}}. \tag{115}$$

The variation in the Hubble function, obtained by numerically solving the system of differential equations Eqs. (111)–(113), is represented for different values of the parameter w of the dark energy equation of state in Fig. 4.
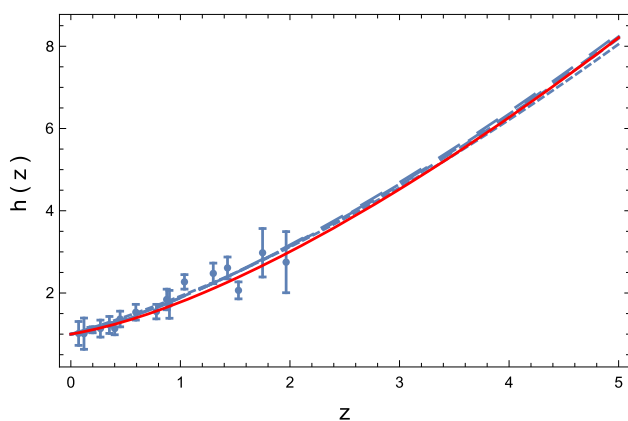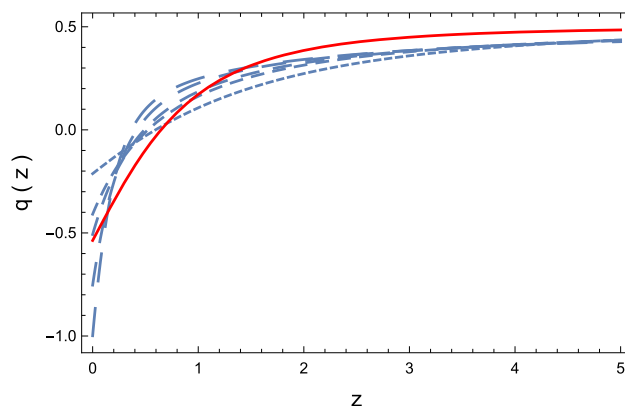
Fig. 4 Variation in the normalized function h as a function of the redshift z in the Barthel–Kropina-FLRW dark energy model for different values of the parameter w of the dark energy equation of state: $w = 1.45$ (short dashed curve), $w = 1.85$ (dashed curve), $w = 2.05$ (long dashed curve), $w = 2.55$ (ultra-long dashed curve), and $w = 3.05$ (ultra-ultra-long dashed curve), respectively. The red solid line represents the prediction of the ΛCDM model. The observational data are represented together with their error bars. The initial conditions used to numerically integrate the system of cosmological evolution equations are $f(0) = 0.33$, $u(0) = 0.51$, and $h(0) = 1$, respectively

Fig. 5 Variation in the deceleration parameter q as a function of the redshift z in the Barthel–Kropina-FLRW dark energy model for different values of the parameter w of the dark energy equation of state: $w = 1.45$ (short dashed curve), $w = 1.85$ (dashed curve), $w = 2.05$ (long dashed curve), $w = 2.55$ (ultra-long dashed curve), and $w = 3.05$ (ultra-ultra-long dashed curve), respectively. The red solid line represents the prediction of the ΛCDM model. The initial conditions used to numerically integrate the system of cosmological evolution equations are $f(0) = 0.33$, $u(0) = 0.51$, and $h(0) = 1$, respectively

Fig. 6 Variation in the density parameter of the matter Ω_m as a function of the redshift z in the Barthel–Kropina-FLRW dark energy model for different values of the parameter w of the dark energy equation of state: $w = 1.45$ (short dashed curve), $w = 1.85$ (dashed curve), $w = 2.05$ (long dashed curve), $w = 2.55$ (ultra-long dashed curve), and $w = 3.05$ (ultra-ultra-long dashed curve), respectively. The red solid line represents the prediction of the ΛCDM model. The initial conditions used to numerically integrate the system of cosmological evolution equations are $f(0) = 0.33$, $u(0) = 0.51$, and $h(0) = 1$, respectively
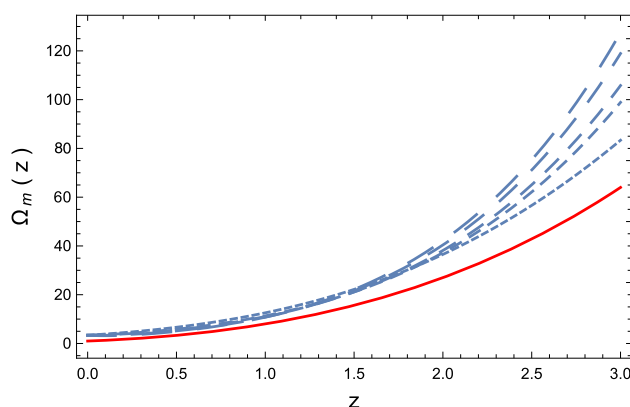
As one can see from Fig. 4, the model gives a good description of the observational data, as well as of the ΛCDM model up to a redshift of at least $z = 5$. For higher redshifts, some differences with respect to the standard cosmology do appear. The numerical results do not show a significant influence of the variation in the parameter of the dark energy equation of state w, with $w = 1.85$ predicting almost the same evolution as $w = 3.05$, but depend strongly on the initial conditions for f and $u = \mathrm{d}f/\mathrm{d}\tau$. The variation in the deceleration parameter as a function of redshift as predicted by the Barthel–Kropina-FLRW dark energy model is presented in Fig. 5.

Even though on a qualitative level the behavior of the deceleration parameter of the Barthel–Kropina-FLRW model can reproduce the predictions of the ΛCDM model, significant quantitative differences still appear. In the Finslerian approach, the evolution of the deceleration parameter is strongly dependent on the parameter w of the dark energy equation of state. At higher redshifts, the numerical values of the Barthel–Kropina-FLRW are slightly lower than those obtained from ΛCDM, and almost independent of w, while at low redshifts the behavior of q essentially depends on the numerical value of w. The critical redshift z_{cr} indicating the transition from deceleration to acceleration, given by $q(z_{cr}) = 0$, also takes numerical values that are different from the ΛCDM predictions. The critical redshift is also strongly dependent on the initial conditions at the present time for f and its derivative.

The density parameter of *the total energy matter content of the universe* is represented as a function of the redshift in Fig. 6. In this case there are significant differences, especially at high redshifts, between the predictions of the Barthel–Kropina-FLRW and the ΛCDM model, with the Finsler type cosmological model predicting much higher matter densities at higher redshifts. In the present model, the matter energy density not only depends on the Hubble function, as in standard general relativity, but also includes the contribution from the one-form field β. Since there is no independent conservation of the matter energy–momentum tensor, the increase in the total matter density at high redshifts can also be interpreted as describing a particle creation process via transfer
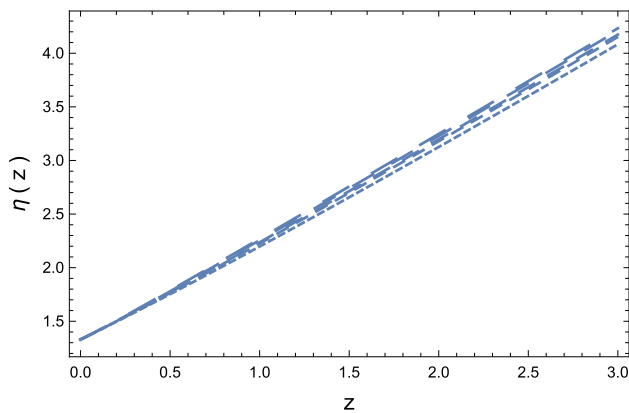
Fig. 7 Variation in the function $\eta(z) = (1+z)(1+f(z))$ as a function of the redshift z in the Barthel–Kropina-FLRW dark energy model for different values of the parameter w of the dark energy equation of state: $w = 1.45$ (short dashed curve), $w = 1.85$ (dashed curve), $w = 2.05$ (long dashed curve), $w = 2.55$ (ultra-long dashed curve), and $w = 3.05$ (ultra-ultra-long dashed curve), respectively. The initial conditions used to numerically integrate the system of cosmological evolution equations are $f(0) = 0.33$, $u(0) = 0.51$, and $h(0) = 1$, respectively

of energy from the η field to ordinary matter, or equivalently, to the increase in the contribution of the dark energy. On the other hand, in the present model we cannot distinguish between baryonic matter, dark matter, and dark energy, and our definition of the density contains all three components. Hence, Ω_m includes the contributions of all matter and energy forms of the universe.

The variation as a function of the redshift of the function η is represented in Fig. 7. The coefficient of the one-form β of the Finsler metric is a monotonically increasing function of z (a monotonically decreasing function of time), and it is a linear function of the redshift. At small redshifts, the evolution of η is almost independent of the numerical values of w, but some small differences do appear at higher redshifts.

6 Discussion and final remarks

In this paper we have investigated the cosmological implications of a particular Finsler type geometry in which the fundamental function is obtained as the ratio of a Riemannian metric α and a one-form β, so that $F = \alpha^2/\beta$. The corresponding geometry is called Kropina geometry, and its properties have been intensively investigated from a mathematical point of view. We have assumed that the physical cosmological metric of the universe is the FLRW metric, from which the metric α^2 is constructed. From a geometric point of view, we have adopted the mathematical formalism of the osculating Finsler spaces, in which the Finsler metric $\hat{g}(x, y)$ is localized via the functional relation $y = y(x)$, and thus a Riemann type metric $g(x, y(x))$ is generated. In our study we have considered A-osculating Riemannian manifolds $\hat{g}(x, A)$, where A_I are the

components of the one-form β. Moreover, we assume that the Finsler space is an n-dimensional point Finsler space (locally Minkowskian but generally non-Euclidean). The connection of a point Finsler space is the Barthel connection, a connection that depends on the field to which it is applied. For an (α, β) metric, the Barthel connection is the Levi–Civita connection of the A-Riemannian metric $\hat{g}(x, A)$. From a physical point of view, we have postulated that the gravitational phenomena can be described by the A-Riemannian metric via the standard Einstein gravitational field equations, in which the Riemannian metric $g(x)$ is substituted by $\hat{g}(x, A)$. Hence, the present approach is based on an extended (but still Riemannian) metric, with the connection and curvature constructed in the standard way.

By adopting as the α metric the standard FLRW form, the generalized Friedmann equations can be obtained by a number of straightforward calculations. Despite the apparent complexity of the mathematical model, the generalized Friedmann equations have a very simple mathematical form, and they are obtained in terms of two geometric quantities, the scale factor a and the component $A_0 = a\eta$ of the one-form β. The generalized Friedmann equations have the remarkable property of giving, in the limit $\eta \to 1/a$, the standard Friedmann equations of general relativity. Thus, the Barthel–Kropina-FLRW model represents a nontrivial deformation of the standard general relativistic cosmology. In the present work we have performed a systematic study of the cosmological properties of the Finslerian type model, which, despite its close relation to standard general relativistic cosmology, also has some very different properties. The generalized Friedmann equations of the Barthel–Kropina-FLRW model do not admit a vacuum solution for $\rho = p = 0$, since the first Friedmann equation gives $\eta' = 0$, $\eta = $ constant, with the second field equation identically satisfied. This situation has some similarities with standard general relativity, in which the vacuum Friedmann equations $3H^2 = (8\pi G/c^2)\rho$ and $2\dot{H}+3H^2 = -(8\pi G/c^4)p$ give for $\rho = p = 0$ the solution $H = 0$, $a = $ constant. Thus, the cosmological background solution of the vacuum gives the Minkowski geometry. On the other hand, in the Brathel–Kropina-FLRW model, the vacuum solution requires $\eta' = 0$, $\eta = $ constant, a condition that does not fix any background spacetime geometry, which remains of the FLRW type, but with arbitrary scale factor a.

However, the model admits a de Sitter type solution for the case of a pressureless cosmological fluid in the presence of a nonzero matter density. The behavior of ρ in this case depends, as one can see from Eq. (73), on an arbitrary integration constant C_1. If this constant is taken as $C_1 = 1$, $\lim_{x^0 \to 0} \rho = \infty$, and therefore the de Sitter evolution begins from a singular state. Finite initial density states are also possible, and in the large time limit, both the matter density and η tend towards some constant values.

In the Barthel–Kropina-FLRW model, the matter energy density is generally not conserved, and the energy density and pressure satisfy the balance equation (65). Conservative cosmological models, obtained by imposing the condition of the energy conservation $\rho' + 3\mathcal{H}\left(\rho c^2 + p\right) = 0$, lead to the standard general relativistic evolution for the scale factor in the presence of matter satisfying a linear barotropic equation of state, $a = \left(x^0\right)^{2/3\gamma}$. Thus, the cosmology of the conservative Barthel–Kropina-FLRW model is identical to the standard general relativistic one. Hence, accelerated expansion is not possible in the presence of matter satisfying the ordinary matter conservation equations. On the other hand, a large number of accelerating cosmological models can be obtained using the general energy balance equation (65), once the functional form of η is fixed. For the sake of the illustration of the qualitative properties of the model, we have considered two particular cosmological scenarios, with $\eta(a) \propto a^{-n}$ and $\eta = \eta(H)$. The first choice of η leads to an eternally accelerating universe, with $q = \text{constant} < 0$, while the second choice leads to a plethora of cosmological models whose properties depend on the choice of the function $\eta(h)$. We have considered and analyzed in detail a particular class of models obtained by choosing $\eta(H) = a_1 H^n + b_1$. The cosmological parameters of this model have been compared with both the observational data and the predictions of the ΛCDM model. Even without the use of a proper fitting procedure for the analysis of the observational data, the Barthel–Kropina-FLRW model can give at least an acceptable qualitative description of the observations of the Hubble function and reproduce the standard ΛCDM model predictions for H. However, significant differences between the Barthel–Kropina-FLRW and the ΛCDM model do appear in the evolution of the deceleration and matter density parameters. In order to test the validity of the present model, a detailed statistical analysis of its predictions with several classes of observational data is necessary.

An effective dark energy model can also be constructed within the framework of the Barthel–Kropina-FLRW geometric theory. Since in the limit $\eta \to 1/a$ one fully recovers the standard Friedmann equations, one can consider small deviations from the standard Friedmann cosmology by adding a correction term f to $1/a$ in the expression of η. This procedure allows the reformulation of the generalized Friedmann equations as the standard ones plus some new terms, which are essentially geometric. They can be interpreted as a geometric dark energy, and they contribute effective energy density ρ_{DE} and pressure p_{DE} terms to the standard baryonic thermodynamic quantities. By imposing a linear equation of state for the dark energy terms, $p_{DE} = w\rho_{DE}$, the system of the cosmological equations can be closed and reformulated as a first-order dynamical system in the redshift space. The solutions of the system can be obtained numerically for different numerical values of the parameter w of the dark energy equation of state and for different initial conditions of the function f and its derivative f'. We have performed a detailed comparison of the solutions of the system with the observational data, and the predictions of the ΛCDM model. The Barthel–Kropina-FLRW model gives a good description of the observational data, and of the ΛCDM model up to at least a redshift of $z = 5$. From the numerical simulations it follows that the numerical values of w have a relatively small influence on the cosmological behavior, which is strongly influenced by the present-day values of f and f'.

Bouncing cosmological models represent an attractive alternative view of the early universe, and many such types of models have been proposed to explain the origin of the universe (see [126] for a review). Bouncing cosmologies have the attractive feature of providing a solution of the singularity problem that generally appears in the standard cosmological models. In the framework of the Finsler and Finsler-like geometries, the problem of the bouncing cosmologies was investigated in [127]. As a first general result, it was shown that in general very special relativity and in Finsler-like gravity on the tangent bundle, the bounce cannot be easily obtained. But in the Finsler–Randers geometry, by adopting for the scale factor the expression $a(t) = a_b\left(1 + Bt^2\right)^{1/3}$, the scalar anisotropy induced by the geometry can satisfy the bounce conditions. Thus, bouncing solutions can be obtained in this class of gravitational theory. In theories constructed by using a nonlinear connection in which a scalar field does appear with an induced scalar–tensor structure, bouncing solutions can also be obtained. Interestingly enough, in the case of the non-holonomic basis, if one imposes to the quantity $N_0(t)$, where $N_\mu \equiv \partial_{\phi^{(\alpha)}} N_\mu^{(\alpha)}$, a specific expression in terms of the scalar field and the Hubble function, then this N_0 can generate the bouncing scale factor.

Bouncing solutions can also be obtained, at least in principle, in the Barthel–Kropina cosmological model. By fixing in advance the form of the scale factor so that it has the required bouncing properties, the generalized Friedmann equations (52) and (53) can be reduced to a (strongly nonlinear) system of differential equations for η, in which the matter energy density and pressure terms are also present. The investigation of this system can be done only by using numerical (or perturbative) methods. However, in order to obtain bouncing solutions, a nonzero matter energy density must be present in the very early universe.

There are at least three possibilities for a possible theoretical understanding of the vast amount of cosmological data that have radically changed our view of the universe. The first approach is called the *dark components model*, and it generalizes the Einstein gravitational field equations by adding two new terms in the total cosmological energy momentum tensor which correspond to dark energy and dark matter,

respectively. In this pathway, the gravitational dynamics are described by the generalized Einstein equation [128]

$$G_{\mu\nu} = \kappa^2 T_{\mu\nu}^{\text{bar}} + \kappa^2 T_{\mu\nu}^{\text{DM}}(\phi, \psi_\mu, \ldots) + \kappa^2 T_{\mu\nu}^{\text{DE}}(\phi, \psi_\mu, \ldots),$$
(116)

where $T_{\mu\nu}^{\text{bar}}$, $T_{\mu\nu}^{\text{DM}}(\phi, \psi_\mu, \ldots)$, and $T_{\mu\nu}^{\text{DE}}(\phi, \psi_\mu, \ldots)$ represent the energy–momentum tensors of baryonic matter, dark matter, and dark energy, respectively. Hence, in this extension of general relativity, dark energy is a form of matter, an interpretation suggested by the equivalence principle of the theory of relativity that states the equivalence of mass and energy. The energy–momentum tensors of dark energy and dark matter can be realized by using scalar or vector fields. The simplest dark constituent model can be obtained by assuming that dark energy is a scalar field ϕ with a self-interaction potential $V(\phi)$. For reviews and extensive discussions of the dark component models see [30–35]).

A second approach to the geometric description of the gravitational interaction is the *dark gravity* approach. The dark gravity formalism assumes a purely geometric description of the gravitational phenomena, and it is based on a modification of the geometric structure of the Einstein field equations, still formulated in a Riemannian geometry. In the dark gravity approach, one can formulate the Einstein gravitational field equations generally as

$$G_{\mu\nu} = \kappa^2 T_{\mu\nu}^{(mat)} + \kappa^2 T_{\mu\nu}^{(\text{geom})}\left(g_{\mu\nu}, R, \Box R, \ldots\right),$$
(117)

where $T_{\mu\nu}^{(\text{geom})}\left(g_{\mu\nu}, R, \Box R, \ldots\right)$ is a term generating a geometrically effective energy–momentum tensor, constructed from the Riemannian metric. The geometric term $T_{\mu\nu}^{(\text{geom})}$ $\left(g_{\mu\nu}, R, \Box R, \ldots\right)$ can describe dark matter, dark energy, or even both. An interesting example of dark gravity is the $f(R)$ theory [113], in which the standard Hilbert–Einstein action $S = \int \left(R/\kappa^2 + L_m\right)\sqrt{-g}\mathrm{d}^4x$ is generalized to an action given by $S = \int \left[f(R)/\kappa^2 + L_m\right]\sqrt{-g}\mathrm{d}^4x$, where $f(R)$ is an arbitrary analytical function of the Ricci scalar R. For reviews of dark gravity theories and their applications, see [117,129–132].

There is a third avenue for the understanding of the present-day cosmological data, called *the dark coupling* theory. In this approach, the standard Hilbert–Einstein Lagrangian density, having a simple additive structure in the geometric and matter Lagrangian, is replaced by a Lagrangian with a more general algebraic system. In the dark coupling theory, one looks for the maximal extension of the standard Hilbert–Einstein gravitational Lagrangian, and this extension can be obtained by assuming that the gravitational Lagrangian density is an arbitrary analytical function of the curvature scalar R describing the geometric properties of the spacetime and the matter Lagrangian L_m. Other thermodynamic or geometric parameters can also be naturally included in specific models. The dark coupling approach leads naturally to the existence of a *non-minimal coupling between curvature and matter*.

In the dark coupling approach, the Einstein gravitational field equations can be formulated as

$$G_{\mu\nu} = \kappa^2 T_{\mu\nu}^{(mat)} + \kappa^2 T_{\mu\nu}^{(\text{coup})}\left(g_{\mu\nu}, R, L_m, T, \Box R, \Box T, \ldots\right),$$
(118)

with the effective energy–momentum tensor of the theory $T_{\mu\nu}^{(\text{coup})}\left(g_{\mu\nu}, R, L_m, T, \Box R, \Box T, \ldots\right)$ obtained by considering the maximal extension of the Hilbert–Einstein Lagrangian. Moreover, a *non-additive curvature–matter algebraic structure* is introduced, describing the couplings between matter and spacetime geometry. The dark coupling theories were considered in [133], where a gravitational action of the form $S = \int \left[f_1(R) + (1 + \lambda f_2(R))L_m\right]\sqrt{-g}\mathrm{d}^4x$ was proposed. This action was generalized in [134] and [134], leading finally to the $f(R, L_m)$ gravity theory [135], in which the gravitational Lagrangian density is given by an arbitrary function of the Ricci scalar and of the matter Lagrangian, $S = \int f(R, L_m)\sqrt{-g}\mathrm{d}^4x$. One can also couple curvature and matter via the trace of the matter energy–momentum tensor, as in the $f(R, T)$ theory, with action given by $S = \int \left[f(R, T) + L_m\right]\sqrt{-g}\mathrm{d}^4x$ [136]. For a detailed presentation of the theories with curvature–matter coupling see [114].

However, a fourth possibility for the description of the gravitational dynamics and evolution, including the accelerating expansion, is also possibly in the framework of the *dark geometry* approach, in which one assumes that the true geometry of the nature is beyond the Riemann one and that the extra terms generated by the non-Riemannian mathematical structures may be responsible for the existence of dark matter and dark energy. One possible dark geometry candidate is Weyl geometry, with conformally invariant gravitational models explaining the present and early dynamics of the universe [137]. In the present work, we have presented another example of a dark geometry, the Finsler type Barthel–Kropina-FLRW geometry, in which an effective dark energy can be generated from the mathematical structures underlying the geometry. The gravitational field equations are postulated as having a similar form as the Einstein equations in Riemann geometry, but with the curvature tensors replaced by their Finslerian counterparts. There is a close relation between the Riemannian cosmological evolution equations and the Finslerian ones, and this relation allows the natural introduction of a geometric dark energy term in the gravitational formalism.

Hence, the Barthel–Kropina-FLRW model not only may represent an attractive alternative to the standard ΛCDM model, but could also open new avenues for the understanding of the complex relation between mathematics and physical reality.

Data Availability Statement This manuscript has no associated data or the data will not be deposited. [Authors' comment: There are no data associated with this article because of its theoretical and formal nature.]

Appendix A: Computation of the Barthel–Kropina metric

1 Method 1

We recall the formula for the fundamental tensor of this Kropina metric in [138]

$$\hat{g}_{IJ}(x, y) = \frac{2\alpha^2}{\beta^2}\epsilon g_{IJ}(x) + \frac{3\alpha^4}{\beta^4}b_I b_J$$
$$- \frac{4\alpha^2}{\beta^3}(\widetilde{g}_{0I}b_J + \widetilde{g}_{0J}b_I) + \frac{4}{\beta^2}\widetilde{g}_{0I}\widetilde{g}_{0J}, \quad \text{(A1)}$$

where $\widetilde{g}_{0I} := \epsilon g_{IJ}y^J$ (see [138]). *Note that the index zero in the $\widetilde{g}$ terms means contraction by y^I.*

Using the above formula, we will compute the components of the metric tensor under the conditions specified below.

Step 1. Assume

(i) $\epsilon = 1$;

(ii) $(g_{IJ}(x)) = \begin{pmatrix} 1 & 0 & 0 & 0 \\ 0 & -a^2(x^0) & 0 & 0 \\ 0 & 0 & -a^2(x^0) & 0 \\ 0 & 0 & 0 & -a^2(x^0) \end{pmatrix}$;

(iii) $(A_I(x)) = \begin{pmatrix} A_0 \\ 0 \\ 0 \\ 0 \end{pmatrix} = \begin{pmatrix} a(x^0)\eta(x^0) \\ 0 \\ 0 \\ 0 \end{pmatrix}$.

Under these assumptions, formula (A1) gives

$$\left(\hat{g}_{IJ}(x, y)\right) = \begin{pmatrix} \hat{g}_{00}(x, y) & \hat{g}_{0i}(x, y) \\ \hat{g}_{0i}(x, y) & \hat{g}_{ij}(x, y) \end{pmatrix}, \quad \text{(A2)}$$

with the components

$$\hat{g}_{00}(x, y) = \frac{2\alpha^2}{\beta^2} + \frac{3\alpha^4}{\beta^4}a^2\eta^2 - \frac{8\alpha^2}{\beta^3}a\eta y^0 + \frac{4}{\beta^2}(y^0)^2,$$

$$\hat{g}_{0i}(x, y) = \frac{4a^2 y^i}{\beta^3}\left(\alpha^2 b_0 - \beta y^0\right),$$

$$\hat{g}_{ij}(x, y) = -\frac{2a^2}{\beta^2}\left[\delta_{ij}\alpha^2 - 2a^2 y^i y^j\right].$$

Observe that on the right-hand side, the indices do not strictly obey the covariant writing form. However, this is not a problem now, since they are more indicative of the position than the summation.

Step 2. We evaluate this matrix for arbitrary x and the specific direction

$$y = (y^I) = A = \begin{pmatrix} A_0 \\ 0 \\ 0 \\ 0 \end{pmatrix} = \begin{pmatrix} a(x^0)\eta(x^0) \\ 0 \\ 0 \\ 0 \end{pmatrix}. \quad \text{(A3)}$$

Then the Kropina fundamental tensor reads

$$\left(\hat{g}_{IJ}(x, y)|_{y=A}\right)$$
$$= \begin{pmatrix} \dfrac{1}{a^2(x^0)\eta^2(x^0)} & 0 & 0 & 0 \\ 0 & \dfrac{-2}{\eta^2(x^0)} & 0 & 0 \\ 0 & 0 & \dfrac{-2}{\eta^2(x^0)} & 0 \\ 0 & 0 & 0 & \dfrac{-2}{\eta^2(x^0)} \end{pmatrix}. \quad \text{(A4)}$$

2 Method 2

Let $\alpha = \sqrt{\epsilon g_{IJ}(x)y^I y^J}$ and $\beta = A_I(x)y^I$, and

$$F = \alpha\phi(s), \quad s = \frac{\beta}{\alpha}, \quad \text{(A5)}$$

The Hessian $\hat{g}$

$$\hat{g}_{IJ} = \epsilon\rho g_{IJ} + \rho_0 b_I b_J + \rho_1(b_I\alpha_J + b_J\alpha_I) - s\rho_1\alpha_I\alpha_J, \quad \text{(A6)}$$

where $\alpha_I := \alpha_{y^I}$ and

$$\rho = \phi^2 - s\phi\phi', \quad \rho_0 = \phi\phi'' + \phi'\phi',$$
$$\rho_1 = -s(\phi\phi'' + \phi'\phi') + \phi\phi'.$$

We obtain first

$$\alpha_I = \alpha_{y^I} = \frac{\partial \alpha}{\partial y^I} = \frac{\partial}{\partial y^I} \sqrt{\epsilon g_{MN} y^M y^N}$$

$$= \frac{1}{2\alpha} \epsilon g_{MN} y^M \delta_I^N + \frac{1}{2\alpha} \epsilon g_{MN} y^N \delta_I^M$$

$$= \frac{1}{2\alpha} \epsilon g_{MI} y^M + \frac{1}{2\alpha} \epsilon g_{IN} y^N$$

$$= \frac{1}{2\alpha} \epsilon y_I + \frac{1}{2\alpha} \epsilon y_I = \epsilon \frac{y_I}{\alpha}.$$

We now consider $y^i = A^i$, then

$$\alpha = \sqrt{\epsilon g_{IJ}(x) A^I A^J} = \sqrt{\epsilon A_I A^J} = \sqrt{\epsilon A^2}$$

$$\beta = A_I A^I = A^2 = \epsilon \alpha^2,$$

$$s = \frac{\beta}{\alpha} = \frac{\epsilon \alpha^2}{\alpha} = \epsilon \alpha, \alpha_I = \epsilon \frac{A_I}{\alpha}.$$

Therefore,

$$\hat{g}_{IJ}(x, A) = \epsilon \rho g_{IJ} + \rho_0 A_I A_J + \rho_1 \left(A_I \epsilon \frac{A_J}{\alpha} + A_J \epsilon \frac{A_I}{\alpha} \right)$$

$$- \epsilon \alpha \rho_1 \epsilon \frac{A_I}{\alpha} \epsilon \frac{A_J}{\alpha}$$

$$= \epsilon \rho g_{IJ} + \rho_0 A_I A_J + 2\epsilon \rho_1 \frac{A_I A_J}{\alpha} - \epsilon \rho_1 \frac{A_I A_J}{\alpha}$$

$$= \epsilon \rho g_{IJ} + (\alpha \rho_0 + \epsilon \rho_1) \frac{A_I A_J}{\alpha}.$$

For the Kropina metric, we let $\phi(s) = \frac{1}{s}$. It follows that

$$\phi'(s) = \frac{-1}{s^2}, \phi''(s) = \frac{2}{s^3}.$$

Therefore,

$$\rho = \frac{2}{s^2}, \rho_0 = \frac{3}{s^4}, \rho_1 = -\frac{4}{s^3}.$$

Substituting $s = \epsilon \alpha$, we obtain

$$\rho = \frac{2}{\alpha^2}, \quad \rho_0 = \frac{3}{\alpha^4}, \quad \rho_1 = \frac{-4}{\epsilon \alpha^3} = \frac{-4\epsilon}{\alpha^3}.$$

Next, we substitute to $\hat{g}(x, A)$, thus obtaining

$$\hat{g}(x, A) = \epsilon \rho g_{IJ} + (\alpha \rho_0 + \epsilon \rho_1) \frac{A_I A_J}{\alpha}$$

$$= \frac{2\epsilon}{\alpha^2} g_{IJ} + \left(\frac{3}{\alpha^3} - \frac{4}{\alpha^3} \right) \frac{A_I A_J}{\alpha}$$

$$= \frac{2\epsilon}{\alpha^2} g_{IJ} - \frac{1}{\alpha^3} \frac{A_I A_J}{\alpha}$$

$$= \frac{1}{\alpha^2} \left(2\epsilon g_{IJ} - \frac{A_I A_J}{\alpha^2} \right). \tag{A7}$$

a Computation of $\hat{g}(x, A)$

Let us now consider the formula (A7) of $\hat{g}(x, A)$ together with the assumptions

(i) $\epsilon = 1$;

(ii) $(A_I) = \left(a \left(x^0 \right) \eta \left(x^0 \right), 0, 0, 0 \right) = (A^I)$;

(iii) $(g_{IJ}) = \begin{pmatrix} 1 & 0 & 0 & 0 \\ 0 & -a^2(x^0) & 0 & 0 \\ 0 & 0 & -a^2(x^0) & 0 \\ 0 & 0 & 0 & -a^2(x^0) \end{pmatrix}$;

(iv) $\alpha|_{y=A(x)} = a(x^0)\eta(x^0)$;

(v) $\beta|_{y=A(x)} = [a(x^0)\eta(x^0)]^2$.

Then we immediately obtain

$$\hat{g}_{00} = \frac{1}{\alpha^2} \left(2g_{00} - \frac{A_0^2}{\alpha^2} \right) = \frac{1}{a^2\eta^2} \left(2 - \frac{(a\eta)^2}{(a\eta)^2} \right)$$

$$= \frac{1}{a^2\eta^2},$$

$$\hat{g}_{ij} = \frac{1}{\alpha^2} \left(2g_{ij} - \frac{A_i A_j}{\alpha^2} \right) = \frac{1}{\alpha^2} \left(2g_{ii} - \frac{A_i^2}{\alpha^2} \right) \delta_{ij}$$

$$= \frac{1}{a^2\eta^2} \left(2(-a^2) \right) \delta_{ij} = -\frac{2}{\eta^2} \delta_{ij}.$$

Hence, the nonvanishing components of $\hat{g}_{IJ}$ are

$$\hat{g}_{IJ} = \begin{cases} \hat{g}_{00} & = \dfrac{1}{a^2(x^0)\eta^2(x^0)}, \\ \hat{g}_{ij} & = \dfrac{-2}{\eta^2(x^0)} \delta_{ij}. \end{cases}$$

Appendix B: Computation of the Christoffel symbols

Recall the formula of Christoffel symbols

$$\hat{\gamma}_{BC}^A = \frac{1}{2} g^{AD} \left(\frac{\partial g_{BD}}{\partial x^C} + \frac{\partial g_{CD}}{\partial x^B} - \frac{\partial g_{BC}}{\partial x^D} \right), \tag{B1}$$

where

$$\hat{g}^{IJ} = \begin{pmatrix} a^2\eta^2 & 0 & 0 & 0 \\ 0 & \dfrac{-\eta^2}{2} & 0 & 0 \\ 0 & 0 & \dfrac{-\eta^2}{2} & 0 \\ 0 & 0 & 0 & \dfrac{-\eta^2}{2} \end{pmatrix}.$$

We begin by computing the derivatives of $\hat{g}_{IJ}$, that is

$$\frac{\partial \hat{g}_{00}}{\partial x^0} = \frac{\partial}{\partial x^0} \left(\frac{1}{a^2(x^0)\eta^2(x^0)} \right)$$

$$= \frac{-1}{a^4\eta^4} (a^2(2\eta\eta') + \eta^2(2aa'))$$

$$= -\frac{2(a\eta' + a'\eta)}{a^3\eta^3},$$

$$\frac{\partial \hat{g}_{ij}}{\partial x^0} = \frac{\partial}{\partial x^0} \frac{-2}{\eta^2(x^0)} \delta_{ij} = \frac{4\eta'}{\eta^3} \delta_{ij}.$$

Next, we compute the Christoffel symbols

$$\hat{\gamma}_{00}^0 = \frac{1}{2} g^{00} \left(\frac{\partial g_{00}}{\partial x^0} + \frac{\partial g_{00}}{\partial x^0} - \frac{\partial g_{00}}{\partial x^0} \right)$$
$$= \frac{1}{2} g^{00} \left(\frac{\partial g_{00}}{\partial x^0} \right) = \frac{1}{2} a^2 \eta^2 \left[-\frac{2(a\eta' + a'\eta)}{a^3 \eta^3} \right]$$
$$= -\frac{(a\eta' + a'\eta)}{a\eta} = -\frac{(\eta\mathcal{H} + \eta')}{\eta},$$

$$\hat{\gamma}_{ij}^0 = \frac{1}{2} g^{0D} \left(\frac{\partial g_{iD}}{\partial x^j} + \frac{\partial g_{jD}}{\partial x^i} - \frac{\partial g_{ij}}{\partial x^D} \right)$$
$$= \frac{1}{2} g^{00} \left(\frac{\partial g_{i0}}{\partial x^j} + \frac{\partial g_{j0}}{\partial x^i} - \frac{\partial g_{ij}}{\partial x^0} \right)$$
$$= \frac{1}{2} g^{00} \left(-\frac{\partial g_{ij}}{\partial x^0} \right) = \frac{1}{2} a^2 \eta^2 \left(-\frac{4\eta'}{\eta^3} \right) \delta_{ij} = \frac{-2a^2 \eta'}{\eta} \delta_{ij},$$

$$\hat{\gamma}_{0j}^i = \frac{1}{2} g^{iD} \left(\frac{\partial g_{0D}}{\partial x^j} + \frac{\partial g_{jD}}{\partial x^0} - \frac{\partial g_{0j}}{\partial x^D} \right)$$
$$= \frac{1}{2} g^{is} \left(\frac{\partial g_{js}}{\partial x^0} \right) = \frac{1}{2} g^{ij} \left(\frac{\partial g_{ji}}{\partial x^0} \right)$$
$$= \frac{1}{2} \left(\frac{-\eta^2}{2} \right) \left(\frac{4\eta'}{\eta^3} \right) \delta_j^i = \frac{-\eta'}{\eta} \delta_j^i,$$

where $\mathcal{H} = \frac{a'}{a}$.

Appendix C: Computation of the Ricci tensor

We start by computing the derivatives of the nonvanishing Christoffel symbols,

$$\frac{\partial}{\partial x^0} \hat{\gamma}_{00}^0 = \frac{\partial}{\partial x^0} \left(\frac{-(a\eta' + a'\eta)}{a\eta} \right)$$
$$= -\frac{a\eta(a\eta'' + a'\eta' + a'\eta' + a''\eta) - (a\eta' + a'\eta)}{a^2 \eta^2}$$
$$\qquad\qquad\qquad\qquad\qquad\qquad (a\eta' + a'\eta)$$
$$= -\frac{a^2 \eta\eta'' + 2aa'\eta\eta' + aa''\eta^2 - a^2(\eta')^2}{a^2 \eta^2}$$
$$\qquad\qquad -2aa'\eta\eta' - (a')^2\eta^2$$
$$= \frac{a^2(\eta')^2 + (a')^2\eta^2 - a^2\eta\eta'' - aa''\eta^2}{a^2 \eta^2},$$

$$\frac{\partial}{\partial x^0} \hat{\gamma}_{ij}^0 = \frac{\partial}{\partial x^0} \left(\frac{-2a^2\eta'}{\eta} \delta_j^i \right)$$
$$= -2\frac{\eta(a^2\eta'' + 2aa'\eta') - a^2(\eta')^2}{\eta^2} \delta_j^i$$
$$= \frac{2a^2(\eta')^2 - 2a^2\eta\eta'' - 4aa'\eta\eta'}{\eta^2} \delta_j^i,$$

$$\frac{\partial}{\partial x^0} \hat{\gamma}_{0j}^i = \left(\frac{-\eta'}{\eta} \delta_j^i \right) = -\frac{\eta\eta'' - (\eta')^2}{\eta^2} \delta_j^i$$
$$= \frac{(\eta')^2 - \eta\eta''}{\eta^2} \delta_j^i.$$

Next, we compute the Ricci tensor. Recall the formula for the Ricci tensor, that is,

$$\hat{R}_{BD} = \sum_A \left[\frac{\partial \hat{\gamma}_{BD}^A}{\partial x^A} - \frac{\partial \hat{\gamma}_{BA}^A}{\partial x^D} + \sum_E \left(\hat{\gamma}_{BD}^E \hat{\gamma}_{EA}^A - \hat{\gamma}_{BA}^E \hat{\gamma}_{ED}^A \right) \right].$$
(C1)

Thus we obtain

$$\hat{R}_{00} = \sum_A \left[\frac{\partial \hat{\gamma}_{00}^A}{\partial x^A} - \frac{\partial \hat{\gamma}_{0A}^A}{\partial x^0} + \sum_E \left(\hat{\gamma}_{00}^E \hat{\gamma}_{EA}^A - \hat{\gamma}_{0A}^E \hat{\gamma}_{E0}^A \right) \right]$$
$$= \sum_A \left[\frac{\partial \hat{\gamma}_{00}^A}{\partial x^A} - \frac{\partial \hat{\gamma}_{0A}^A}{\partial x^0} + \hat{\gamma}_{00}^0 \hat{\gamma}_{0A}^A - \hat{\gamma}_{0A}^0 \hat{\gamma}_{00}^A \right.$$
$$\qquad \left. + 3(\hat{\gamma}_{00}^s \hat{\gamma}_{sA}^A - \hat{\gamma}_{0A}^s \hat{\gamma}_{s0}^A) \right]$$
$$= \sum_A \left[\frac{\partial \hat{\gamma}_{00}^A}{\partial x^A} - \frac{\partial \hat{\gamma}_{0A}^A}{\partial x^0} + \hat{\gamma}_{00}^0 \hat{\gamma}_{0A}^A - \hat{\gamma}_{0A}^0 \hat{\gamma}_{00}^A - 3\hat{\gamma}_{0A}^s \hat{\gamma}_{s0}^A \right]$$
$$= \frac{\partial \hat{\gamma}_{00}^0}{\partial x^0} - \frac{\partial \hat{\gamma}_{00}^0}{\partial x^0} + \hat{\gamma}_{00}^0 \hat{\gamma}_{00}^0 - \hat{\gamma}_{00}^0 \hat{\gamma}_{00}^0 - 3\hat{\gamma}_{00}^s \hat{\gamma}_{s0}^0$$
$$\quad + 3 \left[\frac{\partial \hat{\gamma}_{00}^k}{\partial x^k} - \frac{\partial \hat{\gamma}_{0k}^k}{\partial x^0} + \hat{\gamma}_{00}^0 \hat{\gamma}_{0k}^k - \hat{\gamma}_{0k}^0 \hat{\gamma}_{00}^k \right] - 3\hat{\gamma}_{0k}^s \hat{\gamma}_{s0}^k$$
$$= 3 \left[-\frac{\partial \hat{\gamma}_{0k}^k}{\partial x^0} + \hat{\gamma}_{00}^0 \hat{\gamma}_{0k}^k \right] - 3\hat{\gamma}_{0k}^s \hat{\gamma}_{s0}^k$$
$$= 3 \left[-\frac{(\eta')^2 - \eta\eta''}{\eta^2} + \left(\frac{(a\eta' + a'\eta)}{a\eta} \right) \left(\frac{\eta'}{\eta} \right) - \left(\frac{-\eta'}{\eta} \right)^2 \right]$$
$$= \frac{3}{\eta^2} \left[-(\eta')^2 + \eta\eta'' + (\eta')^2 + \frac{a'\eta\eta'}{a} - (\eta')^2 \right]$$
$$= \frac{3}{a\eta^2} \left[a\eta\eta'' + a'\eta\eta' - a(\eta')^2 \right]$$
$$= \frac{3}{\eta^2} \left[\eta\eta'' + \eta\eta'\mathcal{H} - (\eta')^2 \right],$$

and

$$\hat{R}_{ij} = \sum_A \left[\frac{\partial \hat{\gamma}_{ij}^A}{\partial x^A} - \frac{\partial \hat{\gamma}_{iA}^A}{\partial x^j} + \sum_E \left(\hat{\gamma}_{ij}^E \hat{\gamma}_{EA}^A - \hat{\gamma}_{iA}^E \hat{\gamma}_{Ej}^A \right) \right]$$
$$= \sum_A \left[\frac{\partial \hat{\gamma}_{ij}^A}{\partial x^A} + \hat{\gamma}_{ij}^0 \hat{\gamma}_{0A}^A - \hat{\gamma}_{iA}^0 \hat{\gamma}_{0j}^A + 3 \left(\hat{\gamma}_{ij}^s \hat{\gamma}_{sA}^A - \hat{\gamma}_{iA}^s \hat{\gamma}_{sj}^A \right) \right]$$
$$= \sum_A \left[\frac{\partial \hat{\gamma}_{ij}^A}{\partial x^A} + \hat{\gamma}_{ij}^0 \hat{\gamma}_{0A}^A - \hat{\gamma}_{iA}^0 \hat{\gamma}_{0j}^A - \hat{\gamma}_{iA}^s \hat{\gamma}_{sj}^A \right]$$
$$= \frac{\partial \hat{\gamma}_{ij}^0}{\partial x^0} + \hat{\gamma}_{ij}^0 \hat{\gamma}_{00}^0 - \hat{\gamma}_{i0}^0 \hat{\gamma}_{0j}^0 - \hat{\gamma}_{i0}^s \hat{\gamma}_{sj}^0$$
$$\quad + 3 \left[\frac{\partial \hat{\gamma}_{ij}^k}{\partial x^k} + \hat{\gamma}_{ij}^0 \hat{\gamma}_{0k}^k - \hat{\gamma}_{ik}^0 \hat{\gamma}_{0j}^k - \hat{\gamma}_{ik}^s \hat{\gamma}_{sj}^k \right]$$
$$= \frac{\partial \hat{\gamma}_{ij}^0}{\partial x^0} + \hat{\gamma}_{ij}^0 \hat{\gamma}_{00}^0 + \hat{\gamma}_{i0}^s \hat{\gamma}_{sj}^0$$
$$= \frac{2a^2(\eta')^2 - 2a^2\eta\eta'' - 4aa'\eta\eta'}{\eta^2}$$

$$+ \left(\frac{-2a^2\eta'}{\eta}\right)\left(\frac{-(a\eta' + a'\eta)}{a\eta}\right) + \left(\frac{-\eta'}{\eta}\right)\left(\frac{-2a^2\eta'}{\eta}\right)$$

$$= \frac{2a}{\eta^2}\left(3a(\eta')^2 - a\eta\eta'' - a'\eta\eta'\right)\delta_{ij}$$

$$= \frac{2a^2}{\eta^2}\left(3(\eta')^2 - \eta\eta'' - \eta\eta'\mathcal{H}\right)\delta_{ij}.$$

$$= \frac{2a}{\eta^2}\left[-3a(\eta')^2 + 2a\eta\eta'' + 2a'\eta\eta'\right]$$

$$= \frac{2a^2}{\eta^2}\left[-3(\eta')^2 + 2\eta\eta'' + 2\mathcal{H}\eta\eta'\right].$$

The rest of the components of the Einstein tensor vanish.

Appendix D: Ricci scalar

In this appendix, we will compute the Ricci scalar,

$$\hat{R} = \hat{g}^{IJ}\hat{R}_{IJ}. \tag{D1}$$

We obtain

$$\hat{R} = \hat{g}^{00}\hat{R}_{00} + 3\hat{g}^{ii}\hat{R}_{ii}$$

$$= a^2\eta^2\left(\frac{3}{a\eta^2}\left[a\eta\eta'' + a'\eta\eta' - a(\eta')^2\right]\right)$$

$$+ 3\left(\frac{-\eta^2}{2}\right)\left[\frac{-2a}{\eta^2}\left(-3a(\eta')^2 + a\eta\eta'' + a'\eta\eta'\right)\right]$$

$$= 3a^2\eta\eta'' + 3aa'\eta\eta' - 3a^2(\eta')^2$$

$$- 9a^2(\eta')^2 + 3a^2\eta\eta'' + 3aa'\eta\eta'$$

$$= 6a^2\eta\eta'' + 6aa'\eta\eta' - 12a^2(\eta')^2$$

$$= 6a(a\eta\eta'' + a'\eta\eta' - 2a(\eta')^2)$$

$$= 6a^2\left[\eta\eta'' + \mathcal{H}\eta\eta' - 2(\eta')^2\right].$$

Appendix E: The generalized Friedmann equations

Recall the formula of the Einstein tensor,

$$\hat{G}_{IJ} = \hat{R}_{IJ} - \frac{1}{2}\hat{R}\hat{g}_{IJ}. \tag{E1}$$

It follows that

$$\hat{G}_{00} = \hat{R}_{00} - \frac{1}{2}\hat{R}\hat{g}_{00} = \frac{3}{a\eta^2}\left[a\eta\eta'' + a'\eta\eta' - a(\eta')^2\right]$$

$$- \frac{1}{2}\left(6a(a\eta\eta'' + a'\eta\eta' - 2a(\eta')^2)\right)\frac{1}{a^2\eta^2}$$

$$= \frac{3}{a\eta^2}\left[a\eta\eta'' + a'\eta\eta' - a(\eta')^2 - a\eta\eta'' - a'\eta\eta' + 2a(\eta')^2\right]$$

$$= \frac{3(\eta')^2}{\eta^2},$$

and

$$\hat{G}_{ii} = \hat{R}_{ii} - \frac{1}{2}\hat{R}\hat{g}_{ii} = \frac{2a}{\eta^2}\left(3a(\eta')^2 - a\eta\eta'' - a'\eta\eta'\right)$$

$$- \frac{1}{2}\left(6a(a\eta\eta'' + a'\eta\eta' - 2a(\eta')^2)\right)\left(\frac{-2}{\eta^2}\right)$$

$$= \frac{2a}{\eta^2}\left[3a(\eta')^2 - a\eta\eta'' - a'\eta\eta' + 3a\eta\eta'' + 3a'\eta\eta' - 6a(\eta')^2\right]$$

References

1. P. Finsler, Über Kurven und Flächen in allgemeinen Räumen, Dissertation, Göttingen, JFM 46.1131.02 (1918). Reprinted by Birkhäuser (1951)
2. H. Rund, *The Differential Geometry of Finsler Spaces* (Springer, Berlin, 1959)
3. G.S. Asanov, *Finsler Geometry, Relativity and Gauge Theories* (D. Reidel Publishing Company, Dordrecht, 1985)
4. A. Bejancu, *Finsler Geometry and Applications* (Ellis Horwood, New York, 1990)
5. D. Bao, S.-S. Chern, Z. Shen, *An Introduction to Riemann–Finsler Geometry* (Springer, New York, 2000)
6. Y.-B. Shen, Z. Shen, *Introduction to Modern Finsler Geometry* (World Scientific, Singapore, 2016)
7. S.S. Chern, Not. Am. Math. Soc. **43**, 959 (1996)
8. B. Riemann, Habilitationsschrift, 1854, Abhandlungen der Königlichen Gesellschaft der Wissens?. Chaften zu Göttingen **13**, 1 (1867)
9. G. Randers, Phys. Rev. **59**, 195 (1941)
10. I. Tavernelli, Ann. Phys. **371**, 239 (2016)
11. I. Tavernelli, Ann. Phys. **393**, 447 (2018)
12. S.-D. Liang, S.V. Sabau, T. Harko, Phys. Rev. D **100**, 105012 (2019)
13. I. Tavernelli, Found. Phys. **51**, 46 (2021)
14. A.G. Riess et al., Astron. J. **116**, 1009 (1998)
15. S. Perlmutter et al., Astrophys. J. **517**, 565 (1999)
16. P. de Bernardis et al., Nature **404**, 955 (2000)
17. S. Hanany et al., Astrophys. J. **545**, L5 (2000)
18. R.A. Knop et al., Astrophys. J. **598**, 102 (2003)
19. M. Hicken, W.M. Wood-Vasey, S. Blondin, P. Challis, S. Jha, P.L. Kelly, A. Rest, R.P. Kirshner, Astrophys. J. **700**, 1097 (2009)
20. R. Amanullah et al., Astrophys. J. **716**, 712 (2010)
21. D.H. Weinberg, M.J. Mortonson, D.J. Eisenstein, C. Hirata, A.G. Riess, E. Rozo, Phys. Rep. **530**, 87 (2013)
22. N. Aghanim et al., Planck Collaboration, Astron. Astrophys. **641**, A6 (2020)
23. K.S. Dawson et al., Astron. J. **145**, 10 (2013)
24. K.S. Dawson et al., Astron. J. **151**, 44 (2016)
25. M. Gatti et al., Mon. Not. R. Astron. Soc. **510**, 1223 (2022)
26. A. Einstein, Sitzungsberichte der Königlich Preussischen Akademie der Wissenschaften. Berlin Part **1**, 142 (1917)
27. S. Weinberg, Rev. Mod. Phys. **61**, 1 (1989)
28. H. Martel, P.R. Shapiro, S. Weinberg, Astrophys. J. **492**, 29 (1998)
29. S. Weinberg, The cosmological constant problems, in *Sources and Detection of Dark Matter and Dark Energy in the Universe. Fourth International Symposium, February 23-25, 2000, at Marina del Rey, California, USA*. ed. by D.B. Cline (Springer, Berlin, 2001), p. 18. arXiv:astro-ph/0005265v1
30. A. Joyce, B. Jain, J. Khoury, M. Trodden, Phys. Rep. **568**, 1 (2015)
31. P.J.E. Peebles, B. Ratra, Rev. Mod. Phys. **75**, 559 (2003)
32. T. Padmanabhan, Phys. Rep. **380**, 235 (2003)
33. A. Joyce, L. Lombriser, F. Schmidt, Annu. Rev. Nucl. Part. Sci. **66**, 95 (2016)
34. A.N. Tawfik, E.A. El Dahab, Gravit. Cosmol. **25**, 103 (2019)
35. N. Frusciante, L. Perenon, Phys. Rep. **857**, 1 (2020)

36. B. Ratra, P.J.E. Peebles, Phys. Rev. D **37**, 3406 (1988)
37. P.J.E. Peebles, B. Ratra, Astrophys. J. Lett. **325**, L17 (1988)
38. R.R. Caldwell, R. Dave, P.J. Steinhardt, Phys. Rev. Lett. **80**, 1582 (1998)
39. Y. Fujii, K. Maeda, *The Scalar-Tensor Theory of Gravitation* (Cambridge University Press, Cambridge, 2003)
40. V. Faraoni, *Cosmology in Scalar–Tensor Gravity* (Kluwer Academic Publishers, Dordrecht, 2004)
41. A. Arbey, F. Mahmoudi, Prog. Part. Nucl. Phys. **119**, 103865 (2021)
42. E. Oks, New Astron. Rev. **93**, 101632 (2021)
43. J. de Dios Zornoza, Universe **7**, 415 (2021)
44. P. Salucci, C. Frigerio Martins, A. Lapi (2011). arXiv:1102.1184
45. J. Binney, S. Tremaine, *Galactic Dynamics* (Princeton University Press, Princeton, 1987)
46. M. Persic, P. Salucci, F. Stel, Mon. Not. R. Astron. Soc. **281**, 27 (1996)
47. A. Boriello, P. Salucci, Mon. Not. R. Astron. Soc. **323**, 285 (2001)
48. J.M. Overduin, P.S. Wesson, Phys. Rep. **402**, 267 (2004)
49. V. Beylin, M. Khlopov, V. Kuksa, N. Volchanskiy, Universe **6**, 196 (2020)
50. O. Lebedev, Prog. Part. Nucl. Phys. **120**, 103881 (2021)
51. L. Bian, X. Liu, K.-P. Xie, J. High Energy Phys. **2021**, 175 (2021)
52. S. Alam et al. [BOSS Collaboration], Mon. Not. R. Astron. Soc. **470**, 2617 (2017). arXiv:1607.03155
53. T.M.C. Abbott et al. [DES Collaboration], Phys. Rev. D **98**, 043526 (2018)
54. M. Tanabashi et al. [Particle Data Group], Phys. Rev. D **98**, 030001 (2018)
55. N. Aghanim et al. [Planck Collaboration], Astron. Astrophys. **641**, A6 (2020)
56. A.G. Riess, S. Casertano, W. Yuan, L.M. Macri, D. Scolnic, Astrophys. J. **876**, 85 (2019)
57. C.D. Huang, A.G. Riess, W. Yuan, L.M. Macri, N.L. Zakamska, S. Casertano, P.A. Whitelock, S.L. Hoffmann, A.V. Filippenko, D. Scolnic, Astrophys. J. **889**, 5 (2020)
58. D. Pesce et al., Astrophys. J. Lett. **891**, L1 (2020)
59. J.I. Horvath, Phys. Rev. **80**, 901 (1950)
60. J.I. Horvath, A. Moor, Z. Phys. **131**, 548 (1952)
61. Y. Takano, Lettere al Nuovo Cimento **10**, 747 (1974)
62. Y. Takano, Lettere al Nuovo Cimento **11**, 486 (1974)
63. G.S. Asanov, Found. Phys. **11**, 137 (1981)
64. G.S. Asanov, *Finder Geometry, Relativity and Gauge Theories* (D. Reidel, Dordrecht, 1985)
65. G.S. Asanov, Fortschr. Phys. **39**, 185 (1991)
66. G.S. Asanov, Fortschr. Phys. **40**, 667 (1992)
67. R. Miron, M. Anastasiei, *Vector bundles, Lagrangre spaces, and Applications to the theory of relativity (in Romanian)* (Editura Academiei R. S. Romania, Bucharest, 1987)
68. S. Ikeda, *Advanced Studies in Applied Geometry* (Seizansha, Sgamihara, 1995)
69. S.F. Rutz, Gen. Relativ. Gravit. **25**, 1139 (1993)
70. X. Li, Z. Chang, Chin. Phys. C **34**, 28 (2010)
71. D. Boccaletti, M. di Bari, P. Cipriani, G. Pucacco, Nuovo Cimento B **112**, 213 (1997)
72. G.A. Asanov, Rep. Math. Phys. **59**, 111 (2007)
73. Z. Chang, X. Li, Phys. Lett. B **668**, 453 (2008)
74. P.C. Stavrinos, A.P. Kouretsis, M. Stathakopoulos, Gen. Relativ. Gravit. **40**, 1403 (2008)
75. A.P. Kouretsis, M. Stathakopoulos, P.C. Stavrinos, Phys. Rev. D **79**, 104011 (2009)
76. Z. Chang, X. Li, Chin. Phys. C **33**, 626 (2009)
77. P. Stavrinos, Nonlinear Anal. **71**, e1380 (2009)
78. S.I. Vacaru, Phys. Lett. B **690**, 224 (2010)
79. A.P. Kouretsis, M. Stathakopoulos, P.C. Stavrinos, Phys. Rev. D **82**, 064035 (2010)
80. N.E. Mavromatos, V.A. Mitsou, S. Sarkar, A. Vergou, Eur. Phys. J. C **72**, 1956 (2012)
81. S.I. Vacaru, Int. J. Mod. Phys. D **21**, 1250072 (2012)
82. Z. Chang, M. Li, X. Li, Chin. Phys. C **36**, 710 (2012)
83. S. Basilakos, P. Stavrinos, Phys. Rev. D **87**, 043506 (2013)
84. S. Basilakos, A.P. Kouretsis, E.N. Saridakis, P. Stavrinos, Phys. Rev. D **88**, 123510 (2013)
85. X. Li, Z. Chang, Phys. Rev. D **90**, 064049 (2014)
86. M. Hohmann, Int. J. Mod. Phys. A **31**, 1641012 (2016)
87. M. Hohmann, C. Pfeifer, Phys. Rev. D **95**, 104021 (2017)
88. G. Papagiannopoulos, S. Basilakos, A. Paliathanasis, S. Savvidou, P.C. Stavrinos, Class. Quantum Gravity **34**, 225008 (2017)
89. D. Wang, X.-H. Meng, Phys. Dark Universe **21**, 55 (2018)
90. M. Hohmann, C. Pfeifer, N. Voicu, Phys. Rev. D **100**, 064035 (2019)
91. S. Ikeda, E.N. Saridakis, P.C. Stavrinos, A. Triantafyllopoulos, Phys. Rev. D **100**, 124035 (2019)
92. R. Raushan, R. Chaubey, Eur. Phys. J. Plus **135**, 228 (2020)
93. M. Hohmann, C. Pfeifer, N. Voicu, Eur. Phys. J. C **80**, 809 (2020)
94. C.C. Perelman, Ann. Phys. **416**, 168143 (2020)
95. M. Hohmann, C. Pfeifer, N. Voicu, Universe **6**, 65 (2020)
96. G. Papagiannopoulos, S. Basilakos, A. Paliathanasis, S. Pan, P. Stavrinos, Eur. Phys. J. C **80**, 816 (2020)
97. P. Stavrinos, S.I. Vacaru, Universe **7**, 89 (2021)
98. S. Konitopoulos, E.N. Saridakis, P.C. Stavrinos, A. Triantafyllopoulos, Phys. Rev. D **104**, 064018 (2021)
99. E. Kapsabelis, A. Triantafyllopoulos, S. Basilakos, P.C. Stavrinos, Eur. Phys. J. C **81**, 990 (2021)
100. R. Hama, T. Harko, S.V. Sabau, S. Shahidi, Eur. Phys. J. C **81**, 742 (2021)
101. V.K. Kropina, Nauchn. Dokl. Vyssh. Shkoly. Fiz.-Mat. Nauki **2**, 38 (1959)
102. V.K. Kropina, Uch. Zap. Arkhang. Gas. Ped. Inst. **4**, 111 (1959)
103. W. Barthel, Math. Z. **58**, 358 (1953)
104. W. Barthel, Arch. Math. **4**, 346 (1953)
105. R.K. Tavakol, N. Van den Bergh, Phys. Lett. A **112**, 23 (1985)
106. R.K. Tavakol, Int. J. Mod. Phys. A **24**, 1678 (2009)
107. M. Matsumoto, Tensor, NS **24**, 29 (1972)
108. M. Matsumoto, Rep. Math. Phys. **31**, 43 (1992)
109. S. Bacsó, X. Cheng, Z. Shen, ASPM **48**, 73 (2007)
110. R.S. Ingarden, L. Tamássy, Math. Comput. Model. **20**, 93 (1994)
111. A. Nazim, *Über Finslersche Räume* (Diss, München, 1936)
112. O. Varga, Monatsh. Math. Phys. **50**, 165 (1941)
113. H.A. Buchdahl, Mon. Not. R. Astron. Soc. **150**, 1 (1970)
114. T. Harko, F.S.N. Lobo, *Extensions of f(R) Gravity: Curvature-Matter Couplings and Hybrid Metric Palatini Theory* (Cambridge University Press, Cambridge, 2018)
115. Y. Xu, G. Li, T. Harko, S.-D. Liang, Eur. Phys. J. C **79**, 708 (2019)
116. T. Harko, S. Shahidi (2022). arXiv:2202.06349 [gr-qc]
117. Y.F. Cai, S. Capozziello, M. De Laurentis, E.N. Saridakis, Rep. Prog. Phys. **79**, 106901 (2016)
118. T.M. Guimarães, R. de C.Lima, S.H. Pereira, Eur. Phys. J. C **81**, 271 (2021)
119. D.M. Ghilencea, Phys. Rev. D **101**, 045010 (2020)
120. D.M. Ghilencea, Eur. Phys. J. C **81**, 510 (2021)
121. D.M. Ghilencea, Eur. Phys. J. C **82**, 23 (2022)
122. N. Aghanim et al., Planck 2018 results. VI. Cosmological parameters. Astron. Astrophys. **641**, A6 (2020)
123. O. Lahav, A.R. Liddle, to be published in Rev. Part. Phys. 2022 (2022). arXiv:2201.08666 [astro-ph.CO]
124. M. Moresco, Mon. Not. R. Astron. Soc. **450**, L16 (2015)
125. H. Boumaza, K. Nouicer, Phys. Rev. D **100**, 124047 (2019)
126. M. Novello, S.E.P. Bergliaffa, Phys. Rep. **463**, 127 (2008)
127. G. Minas, E.N. Saridakis, P.C. Stavrinos, A. Triantafyllopoulos, Universe **5**, 74 (2019)
128. T. Harko, F.S.N. Lobo, Int. J. Mod. Phys. D **29**, 2030008 (2020)

129. T.P. Sotiriou, V. Faraoni, Rev. Mod. Phys. **82**, 451 (2010)
130. A. De Felice, S. Tsujikawa, Living Rev. Relativ. **13**, 3 (2010)
131. S. Nojiri, S.D. Odintsov, V.K. Oikonomou, Phys. Rep. **692**, 1 (2017)
132. D. Langlois, Int. J. Mod. Phys. D **28**, 1942006–3287 (2019)
133. O. Bertolami, C.G. Boehmer, T. Harko, F.S.N. Lobo, Phys. Rev. D **75**, 104016 (2007)
134. T. Harko, Phys. Lett. B **669**, 376 (2008)
135. T. Harko, F.S.N. Lobo, Eur. Phys. J. C **70**, 373 (2010)
136. T. Harko, F.S.N. Lobo, S. Nojiri, S.D. Odintsov, Phys. Rev. D **84**, 024020 (2011)
137. D. Ghilencea, T. Harko (2021). arXiv:2110.07056
138. R. Yoshikawa, S.V. Sabau, Geom. Dedicata **171**, 119 (2014)